Separation and Purification Technology 231 (2020) 115883

Contents lists available at ScienceDirect

Separation and Purification Technology

journal homepage: www.elsevier.com/locate/seppur

Investigating opportunities for water-lean solvents in CO_2 capture: VLE and heat of absorption in water-lean solvents containing MEA

Ricardo R. Wanderley, Diego D.D. Pinto, Hanna K. Knuutila*

Department of Chemical Engineering, Norwegian University of Science and Technology (NTNU), NO-7491 Trondheim, Norway

ARTICLE INFO

Keywords:
CO_2 absorption
Water-lean solvents
Hybrid solvents
CO_2 solubility
Heat of absorption

ABSTRACT

A thorough investigation on a set of organic diluents for water-lean solvent formulation has been carried in this work. The performance of aqueous monoethanolamine (MEA) 30 %w/w has been compared to that of mixtures between MEA 30 %w/w and methanol, acetone, monoethylene glycol (MEG), N-methyl-2-pyrrolidone (NMP), tetrahydrofurfuryl alcohol (THFA), sulfolane, cyclopentanone (CC5), furfuryl alcohol and γ-butyrolactone. A small calorimeter was employed to obtain both vapor–liquid equilibrium (VLE) and heat of absorption data. Shifting from an aqueous solvent to a non-aqueous one was observed to have significant implications on the VLE, as all water-lean solvents assessed have lower CO_2 solubility than aqueous MEA. However, the heat of absorption is not much affected. The results of these experiments show the limitations of using most ethers, esters and ketones for water-lean solvent formulation, all stemming from the very low dielectric permittivity of these diluents and the difficulty of the stabilization of the intermediary reaction species between MEA and CO_2 within these systems. Nevertheless, the low volatility of solvents containing MEG, NMP or THFA could offer opportunities for processes with overall less reboiler heat duties than that of ordinary aqueous MEA.

1. Introduction

Amine scrubbing is the most mature among the technologies available for CO_2 capture. This process consists in employing an amine solution to first absorb and then release CO_2 in a pair of columns with a heat exchanger inbetween. Critical parameters affecting its viability are how much CO_2 can be absorbed by the solvent, how much CO_2 can be released, and how much energy is demanded for its regeneration [1]. Table 1 shows the abbreviations and symbols used throughout this work in the discussion of these properties.

Aqueous monoethanolamine (MEA) solutions have historically been chosen as popular solvents for amine scrubbing [2], though alternatives such as N-methyldiethanolamine (MDEA) and other tertiary and hindered amines have long established their position in the market. Both in academia and in the industry there can be found a vast research field looking for suitable amines and amine blends for formulating better absorbents, as can be seen in numerous publications [3,4]. These novel absorbents are, more often than not, aqueous formulations. However, a new generation of solvents, has been emerging since at least the 1970s, though only recently have they really raised interest in the scientific community. These water-lean solvents consist of an amine or amine blend plus an organic diluent, which usually but not always is also a good physical absorbent for CO_2. According to one early investigation [5]: "Hybrid solvent formulations are aimed at marrying the separate advantages of chemical and physical solvents". Both non- and low-aqueous solvents are viable, the only requirement being that there should be an organic diluent in the medium together with the amine.

Comparing to aqueous amine absorbents, there have been few studies on water-lean solvents and even less publications disclosing data regarding their formulations. Aiming at filling this gap, this works presents VLE data of various water-lean solvents and CO_2. Henceforth, a clear distinction between water-lean solvents containing diluents more volatile than water (hereafter shortened to HVS, high-volatility solvents) and those containing diluents less volatile (LVS, low-volatility solvents) is made. This distinction is necessary because the industrial applications with HVS require certain structural modifications in the absorption plant [6] which LVS dispense.

The motivations for choosing the solvents studied in this research were:

i. To analyze at least one HVS with methanol which is already commercially viable as seen by its use in the Amisol Process [7], plus one HVS employing acetone (Section 3.1);
ii. To follow the footsteps of Semenova and Leites [8], who published promising results for water-lean solvents containing NMP, THFA and MEG in their book without releasing enough data for its

* Corresponding author.
E-mail address: hanna.k.knuutila@ntnu.no (H.K. Knuutila).

https://doi.org/10.1016/j.seppur.2019.115883
Received 28 June 2019; Received in revised form 30 July 2019; Accepted 1 August 2019
Available online 03 August 2019
1383-5866/ © 2019 The Authors. Published by Elsevier B.V. This is an open access article under the CC BY-NC-ND license (http://creativecommons.org/licenses/BY-NC-ND/4.0/).

Table 1
Abbreviations and symbols used in this work.

Abbreviation	Meaning
Chemicals	
ACE	Acetone
CC5	Cyclopentanone
FA	Furfuryl alcohol
GBL	γ-butyrolactone
H2O	Water
MEA	Monoethanolamine
MEG	Monoethylene glycol
MET	Methanol
NMP	N-methyl-2-pyrrolidone
SULF	Sulfolane
THFA	Tetrahydrofurfuryl alcohol
Others	
HVS	High-volatility solvents
LVS	Low-volatility solvents
VLE	Vapor-liquid equilibrium
Symbol	Meaning
p	pressure
p_{CO2}	CO_2 partial pressure
α	loading, mol CO_2/mol MEA
δ	Hildebrand solubility parameter
ε	Dieletric permittivity
ΔH	heat of absorption, kJ/mol CO_2

repeatability (Section 3.2 and again Section 3.5);
iii. To study ketones, as they are often seen as promising physical solvents for CO_2 absorption [9] (Section 3.3);
iv. To take a further look into the influence that molecular structure has on solvent properties (Section 3.4).

Additionally, THFA was blended with water in various proportions so that differences between non- and low-aqueous solvents could be better assessed in Section 3.6. Fig. 1 shows the chemical structures of the physical diluents used in this study. In the first row one can see methanol (MET) and acetone (ACE), two very small and volatile molecules, respectively an alcohol and a ketone. In the second row are the heavier molecules with lower vapor pressure. Ethylene glycol (MEG) is a diol, more specifically a glycol. N-methyl-2-pyrrolidone (NMP) is a 5-ringed cyclic amide, also known as a lactam. Tetrahydrofurfuryl alcohol (THFA) is a species derived from furfuryl alcohol (FA), which itself is a furan substituted with an hydroxyalkyl group. Sulfolane (SULF) is a cyclic sulfone found solid at room temperature. In the third and final row one can see the structures of cyclopentanone (CC5) and γ-butyrolactone (GBL), respectively a cyclic ketone and a cyclic ester less volatile than water, and that of the aforementioned furfuryl alcohol.

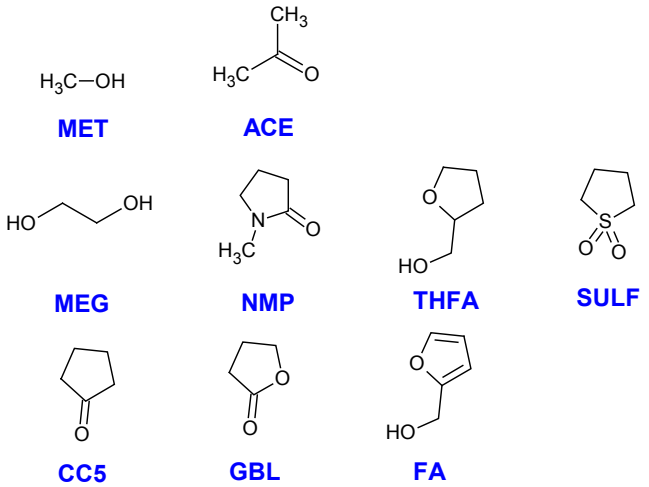

Fig. 1. Chemical structures of the physical diluents used in this study.

Table 2
Physical properties of all chemicals purchased from Sigma-Aldrich and employed in this study.

Chemical	CAS	Purity (%w/w)	Molar mass (g/mol)	Normal boiling point (°C)
MEA	141-43-5	99.0	61.1	170
MET	67-56-1	99.8	32.0	65
ACE	67-64-1	99.5	58.1	56
THFA	97-99-4	99.0	102.1	178
NMP	872-50-4	99.5	99.1	204
MEG	107-21-1	99.8	62.1	198
SULF	126-33-0	99.5	120.2	285
CC5	120-92-3	99.0	84.1	131
FA	98-00-0	98.0	98.1	170
GBL	96-48-0	99.0	86.1	204

2. Methodology

All of the chemicals employed in this study were purchased from Sigma-Aldrich. Other than monoethanolamine (MEA), these include the organic diluents tetrahydrofurfuryl alcohol (THFA), N-methyl-2-pyrrolidone (NMP), monoethylene glycol (MEG), sulfolane (SULF), furfuryl alcohol (FA), methanol (MET), acetone (ACE), cyclopentanone (CC5) and γ-butyrolactone (GBL). Their physical data is shown in Table 2.

Solvents were gravimetrically prepared. A known amount of each organic diluent was poured into a glass bottle on a calibrated scale, after which the necessary quantities of MEA to generate 30 %w/w solvents were added. These solvents were then employed in calorimetric studies. The calorimeter, a CPA202 model provided by ChemiSens AB, consists of a small stirred reactor of approximately 270 cm^3 that is submerged in a bath of diethylene glycol. A schematic drawing of this set-up is displayed in Fig. 2. The operator then sets a determined temperature. After stability is attained, CO_2 kept in a cylinder of approximately 2300 cm^3 is injected in small doses to the bottom of the reactor. Pressure and temperature are measured both in the stirred cell and in the CO_2 vessel, while the temperature control provides that the set point be reached again. By keeping a log of the power input to the reactor, it is possible to obtain a good measure of the CO_2 differential heat of absorption. Through mass balance using pressure-temperature data plus an Equation of State (in this work, Peng-Robinson), vapor-liquid equilibrium (VLE) data is readily obtained. In addition, CO_2 determination of the final loaded solution with the aid of a TOC is employed to make sure that the mass balance obtained in this procedure is reliable. The raw data gathered allows for the calculation of total pressure versus CO_2 loading (α) curves. Other studies that adopted a similar outline are those by Kim and Svendsen [10], Svensson et al. [11] and Evjen et al. [12].

Due to the low sensitivity of the pressure meters at low pressures, the pressure data at the start of the process (when CO_2 partial pressure is below c.a. 5 mbar) is highly inaccurate. As so, it is not possible to obtain reliable CO_2 partial pressure (p_{CO2}) data at low loadings. However, after the maximum stoichiometric loading is achieved, it is reasonable to say that p_{CO2} may be consistently estimated with data available from the experiment.

For the viscosity data presented in Section 3.2, the water-lean solutions were fully loaded with pure CO_2 at room temperature (~20 °C) and then diluted with lean solvent in different proportions for obtaining samples with multiple loading points. These samples were then taken to an Anton Paar Physica MCR 100 viscosity meter and had their viscosities measured at 40 °C, in a procedure similar to that employed by Evjen et al. [13]. Through automatized CO_2 determination of key samples in a TOC apparatus, both before and after the viscosity analysis, it was asserted that not more than 3% CO_2 is desorbed by this procedure and that data thus obtained is reliable.

All of the VLE and heat of absorption data obtained in this work is presented with their corresponding confidence intervals in Appendix A.

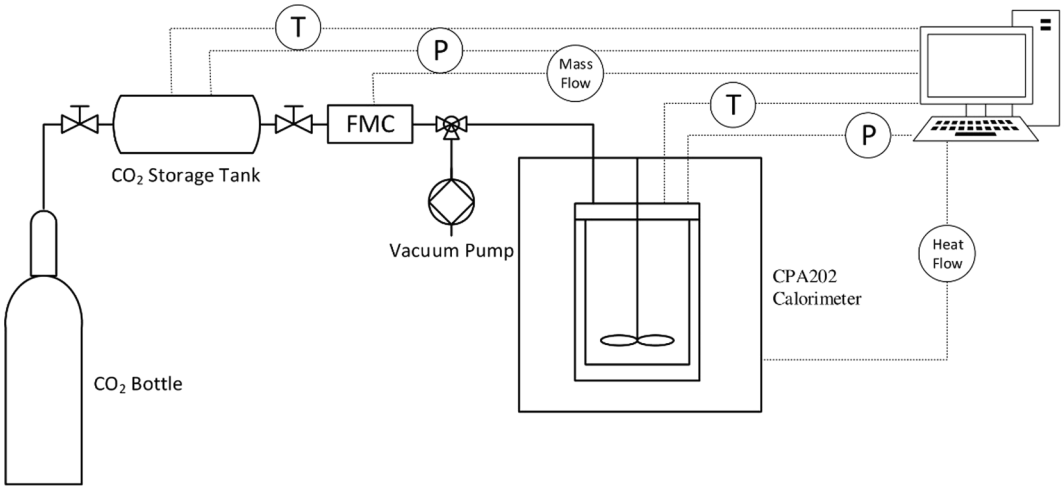

Fig. 2. Experimental set-up employed for the gathering of VLE data.

Appendix B outlines how these confidence intervals are calculated. It is important to underline that the intervals reported refer to the inherent uncertainties of data gathering (i.e. the precision of the readings), and not to the experimental reproducibility of the operational routines. Therefore, error sources such as human mistakes, apparatus malfunctions or unknown disturbances are disregarded. To acknowledge this, a short discussion on reproducibility is given in Appendix C. The reproducibility of heat of absorption is estimated by the average absolute relative deviation (AARD) of 4% for all solvents evaluated in Appendix C, whereas the reproducibility of the VLE data is estimated by the AARD of 8.4% for aqueous MEA. The repeatability of the experiments is evaluated as good by comparison with literature data both on VLE [14,15] as on heat of absorption [10,16].

3. Results and discussion

3.1. High-volatility water-lean solvents (HVS): acetone, methanol

The first class of water-lean solvents assessed in this work is that of high-volatility water-lean solvents, or HVS. Here, this means methanol + MEA and acetone + MEA. Luckily, the mixture of methanol + MEA is a very standard one in the field of water-lean solvents, and plenty of data regarding this combination can be found in the literature. Studies on methanol + MEA mixtures span from Semenova and Leites [8] to the latest works of Usubharatana and Tontiwachwuthikul [17] and Fu et al. [18] among many others. This is, after all, the formulation employed by the classic Amisol Process [7]. Therefore, before presenting the data obtained in this analysis, a short discussion on the available information is warranted. While multiple sources highlight the extended absorption capacity of MEA-methanol mixtures [17,19,20], it is important to notice that operations with HVS pose some peculiarities. These involve the necessity of carrying the process under lower temperatures, of employing a water wash to capture vaporized solvent, of installing a rectification column to adjust the solvent composition, of operating with higher recirculation rates [6,7,21]. All these are consequences of the fact that loss of solvent is critical when employing a volatile organic diluent. Moreover, while all authors mention that MEA-methanol mixtures have less capacity for CO_2 absorption at lower CO_2 partial pressures, they also imply that this behavior is reversed at relatively high CO_2 partial pressures, as an effect of the extended capacity for physical absorption in water-lean solvents. That is to say, a certain "cross-over pressure" should be observed in the VLE data for these solvents.

Fig. 3 shows the capacity for CO_2 absorption presented by the HVS methanol + MEA 30 %w/w, in which the dependency of α with total

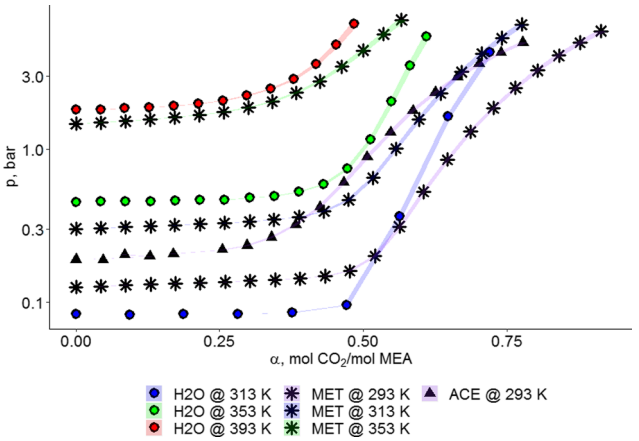

Fig. 3. Semilog plot of total pressure versus loading data for water (H2O), methanol (MET) and acetone (ACE) with MEA 30 %w/w, where the confidence interval for the calculated α is given by the horizontal span of the colored ribbons following the curves.

pressure is more evident than it is in the LVS as will be discussed later. A VLE curve for the aqueous 30 %w/w MEA and the previously untested HVS acetone + MEA 30 %w/w is also present.

In Fig. 3, one can see the VLE curves for aqueous MEA at 313, 353 and 393 K represented by the scattered ○ respectively in blue, green and red. These curves start out flat, indicating that chemical absorption is predominant, i.e. that all CO_2 injected into the calorimeter is absorbed with no increase in the reactor pressure. At around α ≈ 0.50, all amine in the medium has already reacted and the pressure begins to increase with loading. Furthermore, the capacity for CO_2 absorption decreases with increasing temperatures, and thus the curves follow from left to right in the order red ○ (393○ K) → green ○ (353 K) → blue ○ (313 K). Additionally, one should notice that the height of the flatline for these curves increase in the order blue ○ (313 K) → green ○ (353 K) → red ○ (393 K). This happens because what is shown in Fig. 3 is the total pressure measured in the reactor, and the volatility of all solvents increase with temperature, meaning that more solvent will be present in the vapor phase as one moves from 313 K to 393 K. It is worthwhile understanding these trends, since they are repeated for each new set of solvents studied in the course of this work.

One can now observe the VLE curves for methanol + MEA (scattered *) and acetone + MEA (scattered ▲). At any fixed temperature, the curves for methanol not only lie to the left of the ones for aqueous MEA (compare blue ○ to blue * for data at 313 K, or green ○ to green *

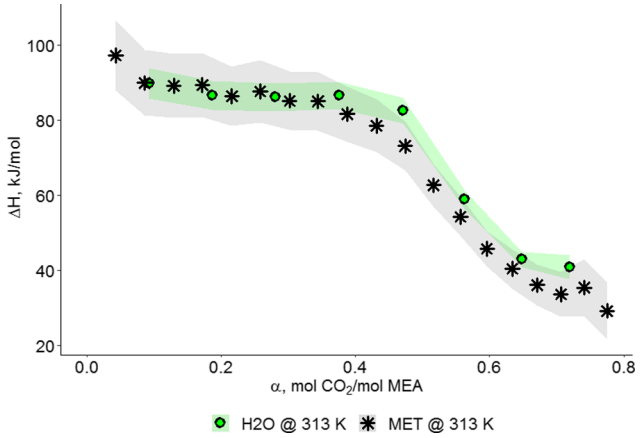

Fig. 4. Differential heat of absorption versus loading data for methanol + MEA 30%w/w, where the confidence interval for the calculated ΔH is given by the vertical span of the colored ribbons following the curves. The heat of absorption curve for aqueous MEA 30 %w/w is also present for comparison purposes.

for data at 353 K), but they also lie above it, meaning that methanol + MEA is more volatile and has less capacity for CO_2 absorption than aqueous MEA. However, the methanol + MEA capacity for CO_2 absorption at 313 K (blue *) apparently surpasses that of the aqueous solution (blue ○) under a total pressure of approximately 4.4 bars, seen where both blue curves meet. Another crossover would probably be observable at 353 K if higher total pressures were studied, as the two green curves seem to converge. This is due to the extended physical absorption properties of water-lean solvents after the stoichiometric loading capacity is exhausted. The fact that this crossover pressure seems to be increasing with temperature may be seen as an indicator that, at least for this particular solution, physical absorption is more affected by changes in temperature than chemical absorption. However, it must be mentioned that this crossover point appears at a relatively high pressure whereas Banasiak [19] found it at approximately 2.25 bars at 30 °C and Usubharatana et al. [20] found it close to 3 bars at an undisclosed temperature.

The heat of absorption for methanol + MEA 30 %w/w at 313 K was compared to that of aqueous MEA in Fig. 4. Given the uncertainties associated with the gathering of data, it is reasonable to conclude that both solutions have similar heat of absorptions at a fixed temperature. This will be seen also for the LVS. Nevertheless, one remarkable fact of water-lean solvents is that their heat of absorption drops faster than that of aqueous solutions at higher loadings. This can be seen by checking that the grey curve in Fig. 4 dives under the green curve at a loading of approximately $\alpha \approx 0.50$. This could be an effect of the extended absorption of CO_2 in aqueous MEA being driven by bicarbonate formation whereas that of MEA-methanol solutions is carried by physical absorption, the former process releasing more heat than the latter.

The solvent acetone + MEA 30 %w/w has a very different performance than the MEA-methanol solution. One can see initially that its VLE curve at 293 K (purple ▲) falls to the left of that of methanol + MEA at 293 K (purple *), signifying less capacity for CO_2 absorption. Moreover, after absorption a phase separation was clearly observed, with the lower phase being a thick gel of orange coloration. This phase separation has implications for the heat of absorption measured in the calorimeter. However, this result will be discussed in Section 3.3 together with that for another ketone + MEA blend due to the similarity of phenomena.

3.2. Low-volatility water-lean solvents (LVS): MEG, NMP, THFA and sulfolane

Moving on from HVS, one arrives at LVS water-lean solvents, of which there are less examples to have been extensively studied in the literature and few cases of industrially standardized formulations (the Sulfinol solvent being the only exception). Nevertheless, the combinations of MEA and MEG, NMP or THFA were all studied by Semenova and Leites [8], while Woertz [22] before them had already considered NMP + MEA and multiple authors thereafter tried some combinations with either one of these diluents and MEA [23–25]. In fact, Semenova and Leites [8] published pilot-plant data that can be useful for comparison with results obtained in the present study.

A very similar discussion on Fig. 5 will be carried as it was done for Fig. 3. Once again, the VLE curves for aqueous MEA (scattered ○) at 313, 353 and 393 K (respectively blue, green and red) are compared to

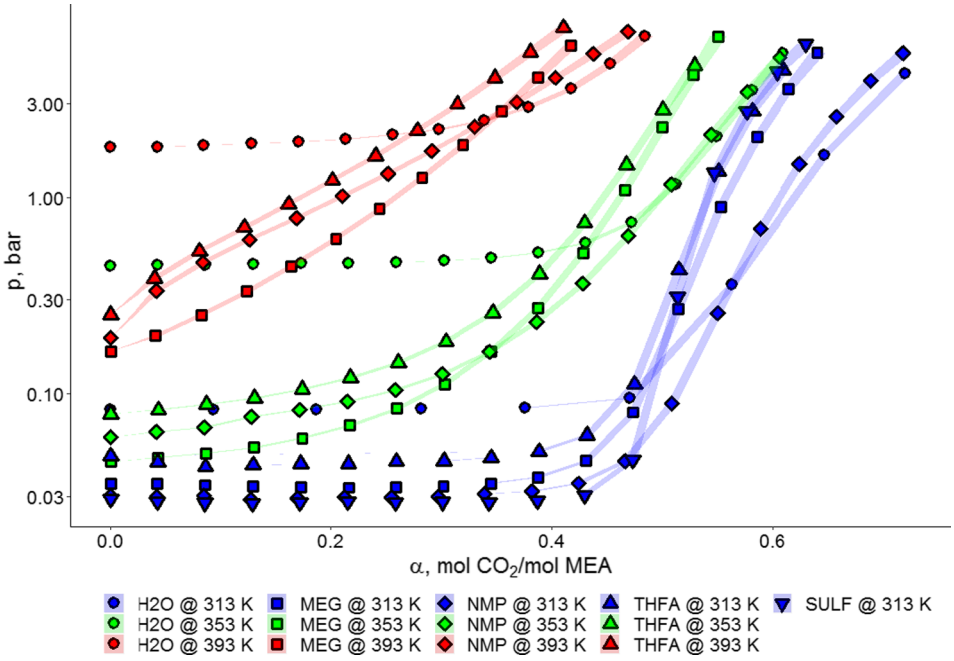

Fig. 5. Semilog plot of total pressure versus loading data for different LVS with MEA 30 %w/w, where the confidence interval for the calculated α is given by the horizontal span of the colored ribbons following the curves. The VLE curve for aqueous MEA 30 %w/w is also present for comparison purposes.

the ones obtained for MEG (scattered □), NMP (scattered □), THFA (scattered △) and sulfolane (scattered ▽). As seen on Fig. 5, the CO_2 capacity of the LVS increases in the order sulfolane < THFA < MEG < NMP at every temperature screened, all of them absorbing less CO_2 than aqueous MEA 30 %w/w. This is clearly evidence by the order in which each curve appears from left to right at any given color (▽ → △ → □ → □ → ○). Additionally, the low-volatility of these solvents is evidenced by comparison between the height of the flatline of the hybrids and that of aqueous MEA at 393 K, before any CO_2 injection is made. At that temperature, aqueous MEA was found to have a vapor pressure of approximately 1.80 bars, in stark contrast to THFA (0.25 bar), NMP (0.19 bar) and MEG (0.16 bar).

The absorption of CO_2 with the water-lean solvent sulfolane + MEA 30 %w/w at 313 K initiated the formation of a second, moderately dense and viscous phase. This is curious, given that several authors [22,23,26] studied mixtures of these substances, many employing aqueous mixtures while one [23] employed a non-aqueous solution, none of them mentioning this phenomenon. It must also be noted that this phase separation has been observed by the present authors also with aqueous blends of sulfolane and MEA in Wanderley et al. [27].

Fig. 6 shows the heat of absorption for the different LVS at 313 K. The curve for sulfolane + MEA 30 %w/w is omitted for an easier visualization, but it would overlap with that for NMP + MEA 30 %w/w. In fact, given the confidence intervals, a certain overlap is seen among all different solvents. This behavior has been observed also at 353 and 393 K, though for those cases the confidence intervals are even wider. This clearly evidences, as it was the deal with methanol + MEA 30 %w/w, that the heat of absorption for water-lean solvents with a fixed amine at a fixed temperature is quite similar to that of the corresponding aqueous solvent. A difference can surely be perceived at higher loadings due to physical absorption rather than bicarbonate formation being the mechanism for CO_2 capture after $\alpha \approx 0.50$ (notice how the green ○ scatter finishes above all the others in the right-hand side of Fig. 6), but while direct reaction between MEA and CO_2 is the main driving force for absorption, there is little difference in the heat released.

A further discussion on the results obtained in this section will be carried in Section 3.5. First and foremost, however, an interesting issue on the functionality of organic solvents must be assessed in Sections 3.3 and 3.4.

3.3. Ketones: acetone, cyclopentanone

There are good reasons for studying ketones as diluents for hybrid solvents. As a class of organic compounds, they are said to be good physical absorbents for CO_2 capture [9,28]. This comes from the fact that their Hildebrand solubility parameter δ is relatively low. According to Gwinner et al. [9], δ is a measure of how strongly connected are the molecules of the solvent. A good CO_2 physical absorbent should not have very high δ, because, as CO_2 molecules are trapped into the solvent, solvent-solvent bonds must be broken so that solvent-CO_2 bonds are created.

On the other hand, as the solubility parameter seems to be strongly related to the dielectric constant ε [29], this means that ε in ketones is also quite small. As previously shown [26,27,30–32], there seems to be a strong correlation between ε and the capacity a solvent has for stabilizing its electrolytic species. Leites [26] goes as far as to say that solvents with $\varepsilon < 10$ are unsuitable for water-lean solvent formulation, solvents with $\varepsilon > 23$ are proper and solvents with $10 < \varepsilon < 23$ fall in a grey zone. All ketones analyzed have $10 < \varepsilon < 23$. In effect, it has become clear that there are two solvent interactions in play when assessing an organic diluent. The first is how well it physically dissolves CO_2, which is related to having a low δ and a low ε. The second is how well it stabilizes the transition compounds formed by the amine plus CO_2 after absorption takes place, which is related to having a high ε. Therefore, if both phenomena are taken into consideration, there should be an optimum ε that guarantees good solvent performance both physically and chemically. In the spectrum of ε, ketones have lower values than the other compounds studied so far. Experiments with them are important to check if the gains by facilitated physical absorption surpass the losses of a troubled chemical interaction.

A HVS and a LVS ketone were selected for the calorimetric experiments. The volatile one is acetone, the smallest ketone and one of the components more structurally similar to CO_2 itself. For this reason, in Fig. 3 the VLE data of acetone + MEA 30 %w/w is compared to that of methanol + MEA 30 %w/w. The non-volatile is cyclopentanone (CC5), which has high boiling point (130.6 °C) and a structure very similar to γ-butyrolactone, which has already been tested and proven as an interesting physical solvent for CO_2 capture [33]. The VLE curve of CC5 + MEA 30 %w/w is compared to that of aqueous MEA in Fig. 7, where aqueous MEA is represented by scattered ○ and CC5 + MEA is represented by scattered ■.

In Fig. 7, the VLE curves with scattered ■ fall always to the left of the ones with scattered ○ at each color, i.e. at each temperature. This implies inferior absorption capacities. In fact, the CO_2 absorption capacity of both acetone (see Fig. 3) and CC5-based water-lean solvents is not only inferior to that of aqueous MEA 30 %w/w, it is also inferior to the remainder water-lean solvents mentioned previously (with methanol, MEG, NMP, THFA and sulfolane). More interestingly though, as can be checked on Fig. 8, both HVS water-lean solvents presented the formation of a very dense and viscous second phase after CO_2

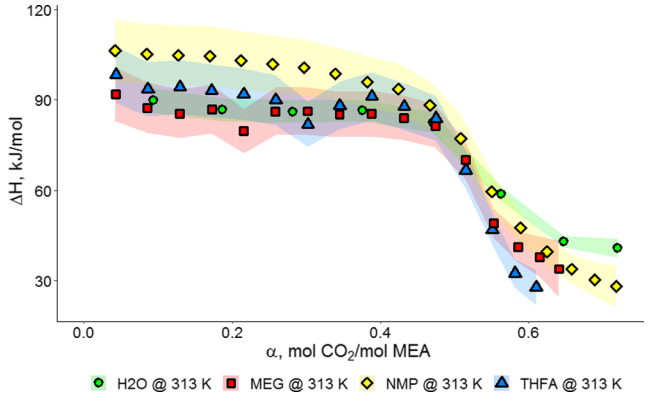

Fig. 6. Differential heat of absorption versus loading data for different LVS with MEA 30%w/w, where the confidence interval for the calculated ΔH is given by the vertical span of the colored ribbons following the curves. The heat of absorption curve for aqueous MEA 30 %w/w is also present for comparison purposes.

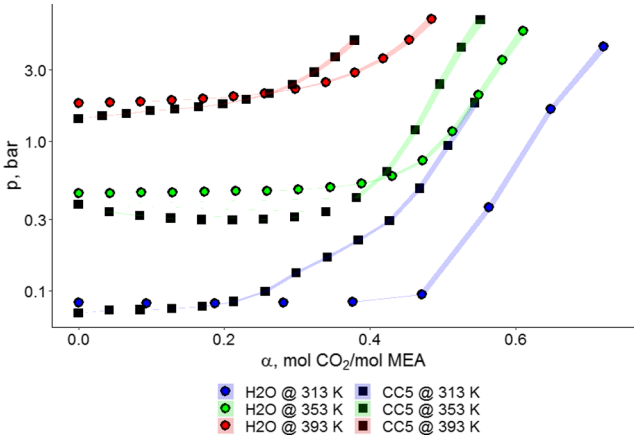

Fig. 7. Semilog plot of total pressure versus loading data for CC5 + MEA 30 %w/w, where the confidence interval for the calculated α is given by the horizontal span of the colored ribbons following the curves. The VLE curve for aqueous MEA 30 %w/w is also present for comparison purposes.

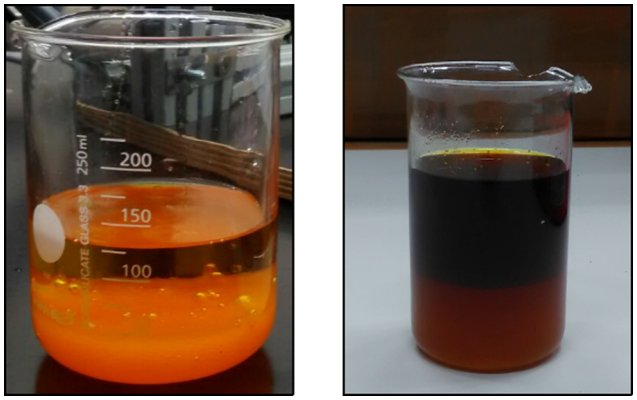

Fig. 8. Phase separation observed respectively in acetone and CC5-based water-lean solvents with 30 %w/w MEA upon CO_2 absorption.

absorption. Furthermore, for CC5, this separation was even more evident at higher temperatures. This could be a direct result of the low polarity of these ketones, but it can also indicate that some reaction, such as the aldol reaction, is taking place between the diluent and the amine. If that would be the case, then the enolization of the diluent would be followed by its condensation reaction, a reaction that is typically benefited by high temperatures and basic environments. This mechanism can be observed in Fig. 9 as adapted from [34], though no analytical routines have been carried so far to properly identify the species obtained in these experiments. Nevertheless, the occurrence of chemical reaction would certainly help explaining the pitch-black colour of the less dense phase observed on the right-hand side of Fig. 8. Additionally, since the experimental procedure with the calorimeter involves stripping the solvent at the start of the routine and then

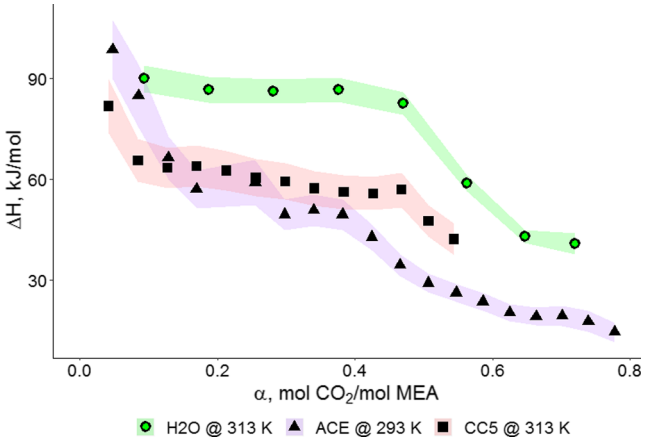

Fig. 10. Differential heat of absorption versus loading data for different ketones with MEA 30%w/w, where the confidence interval for the calculated ΔH is given by the vertical span of the colored ribbons following the curves. The heat of absorption curve for aqueous MEA 30 %w/w is also present for comparison purposes.

injecting pure CO_2 into the reactor, only a negligible amount of dissolved O_2 should be present at any time. One can therefore probably disregard its effects on the side reactions happening in the solvent.

Fig. 10 shows the differential heat of absorption with ketones + MEA 30 %w/w. It is remarkable that the heat of absorption with these water-lean solvents is lower than that of aqueous MEA, as both the purple ▲ scatter and the pink ■ scatter fall below the green ○ scatter. This could be an indication that CO_2 transfer occurs mostly through physical absorption, as the diluents have a dielectric permittivity too low to provide proper carbamate stabilization. Another

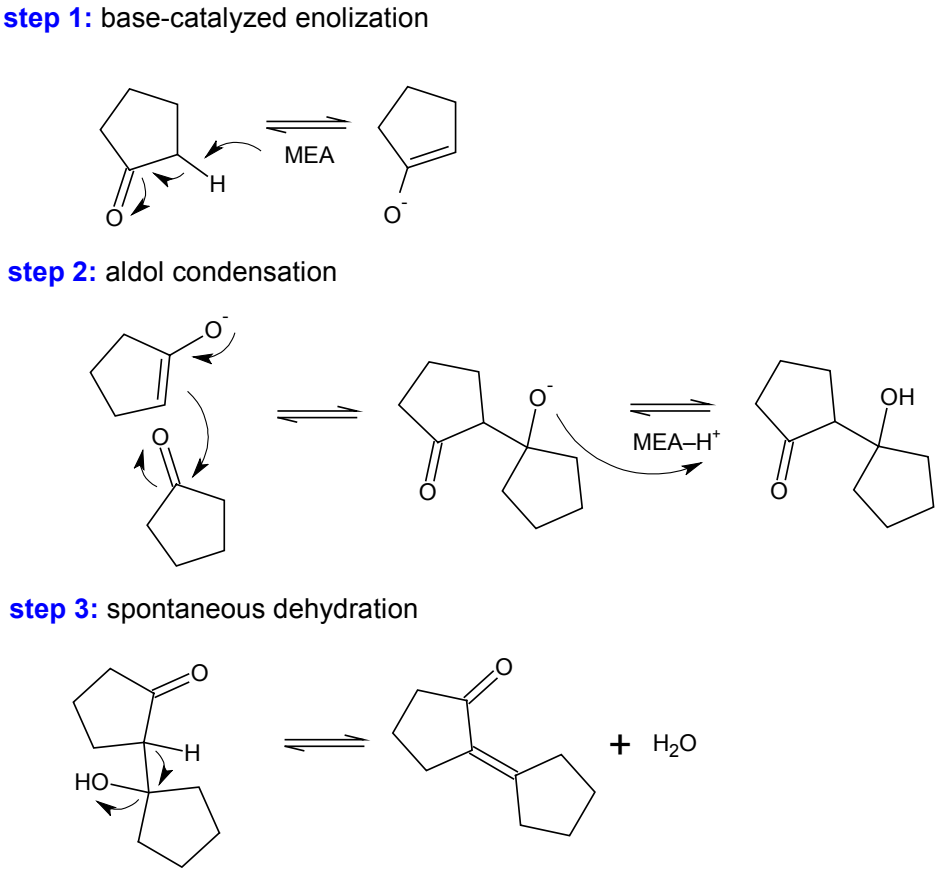

Fig. 9. Proposed reaction mechanism for ketones (e.g. cyclopentanone) and MEA as adapted from [34].

evidence of this is the formation of two phases upon absorption, one upper phase containing the diluent and one lower phase possibly containing the reacted amine, which can be promptly observed by checking the solvent after its removal from the calorimeter (the yellowish coloration of the bottom-phase being a good indication that the MEA-containing species are in that layer). Supporting this hypothesis is the high heat of absorption verified upon first loading at higher temperatures for cyclopentanone + MEA 30 %w/w (see Table A2), typical of phase transition. Alternatively, it could also happen that a reaction other than MEA-carbamate formation accounts for CO_2 absorption in these solvents. Regardless, this class of solvents containing ketones is deemed probably unstable for industrial applications, because if these loaded solutions are left to rest each in a closed glass bottle, after a few days they display a vibrant green coloration, strongly indicating that some unexpected reaction is happening in the solvent.

It would be worth pondering whether ketones with unsaturated α-carbons could provide a less reactive diluent for water-lean solvent formulation, since they would be less prone to enolization (which requires saturated α-carbons to occur) and, consecutively, to the aldol reaction. At any rate, these chemicals are more complex and expensive, and have not been considered any further in this analysis.

3.4. Structure and functionality: FA vs. THFA, GBL vs. CC5

Following the functionality analysis presented in Section 3.3, it is interesting to study the influence that the molecular structure of the organic diluent has on water-lean solvent properties. A first opportunity for this was thought to come up by analyzing the performances of CO_2 absorption with furfuryl alcohol (FA) water-lean solvents and comparing them to those of THFA. The chemical structures of both compounds can be seen in Fig. 1. On account of the resonance phenomenon found in FA, due to the unsaturated carbons in its furan ring, its oxygen is less basic than that of THFA [35], leading to speculations that its dielectric properties would also be weaker. Contrary to this, the only reference found disclosing the ε of both FA and THFA incidentally concludes that the ε of THFA is lower than that of FA [36]. Unfortunately, the same article presents a value for the ε of furfural so different from that of more undisputed sources [37] that the reliability of its conclusions becomes questionable. More properties of these compounds can be found in Table 2.

Similarly, after running the investigation with CC5 + MEA 30 %w/w described previously, it was natural to examine the organic diluent γ-butyrolactone (GBL) as well. GBL has similar properties to CC5, and has also been already described as a good physical absorbent for CO_2 capture [33]. Furthermore, as GBL is an ester and CC5 is a ketone, comparison between both of their results could offer a glimpse on the effects of different organic functions in water-lean solvent formulation for CO_2 capture. The structures of these components can also be seen in Fig. 1, and physical properties can be found in Table 2.

Unfortunately, both analyses have been inconclusive. The capacity of the water-lean solvent FA + MEA 30 %w/w at any given CO_2 partial pressure was far lower than that of the THFA solvent, showing a maximum loading perceptively below $\alpha \approx 0.50$ (see Appendix A). This suggests that some sort of reaction/interaction may be happening that consumes/blocks many of the amine molecules, preventing them from reacting with CO_2. Similarly, GBL + MEA 30 %w/w proved to be a disastrous combination. The solution begins to heat up abnormally as soon as the substances are brought into contact, and CO_2 capture with the resulting water-lean solvent shows no chemical absorption behavior whatsoever. No phase separation was directly observed through the course of these experiments in either water-lean solvents. As in the case of the reaction with ketones mentioned previously, there is yet a lack of information regarding which reaction really occurs between these organic compounds and MEA, and one can merely suggest likeable possibilities to explain the observed phenomena. For the same reasons as stated before, the presence of dissolved O_2 in the solvent should be negligible.

According to Yamamoto et al. [38], feasible diluents for hybrid solvents can be found among the following organic functions: alcohols, esters, ethers and ketones. After the occurrence with GBL, it pays to examine these functions more attentively [34].

- With alcohols, there are no obvious necessary side reactions between diluent and amine that jeopardize the CO_2 absorption process. Alcohols employed in this analysis were methanol, THFA and MEG, the latter being a dialcohol (glycol).
- On the other hand, it is known that the reaction between esters and amines may produce amides or, depending on the water content of the medium, esters may suffer hydrolysis and generate acids. One of these mechanisms, probably the former, may have been responsible for the event observed with GBL.
- Ethers could be fine for hybrid solvent formulation, but it must be noticed that there is risk of peroxide formation under high temperatures. For this reason, the solvent is especially prone to degradation. An ether that was analyzed in this work was THFA. Most ordinary ethers, however, have very low ε.
- Most ketones are liable to suffer enolization and consequent aldol condensation, a process catalyzed by basic media. Both ketones analyzed in this work have α-hydrogens and flexible structures, being susceptible to these reactions.

As a final side note, phase separation in itself is a consequence of salt formation during the reaction between amine and CO_2 and the diluent being unable to solubilize such products. Therefore, even if a suitable non-reactive organic diluent is selected from the functions listed above, its dielectric properties (ε) will define whether it can work as diluent without resulting in phase separation. A discussion on the relationship between ε and water-lean solvent formulation has been carried by several authors [26,30,31] and more recently by Wanderley et al. [27].

3.5. A further look into LVS: Could these solvents deliver lower reboiler heat duties?

An in-depth discussion should be made over the important results obtained in Section 3.2, which showed the most promising results in this study. If one were to break down the processes involved in CO_2 absorption by a chemical solvent, these would be respectively:

1. Opening of a void in the solution, meaning that the solvent molecules need to make space for the incoming CO_2 molecule by breaking their solvent-solvent bonds (endothermic);
2. Subtraction of a CO_2 molecule from the vapor phase, implying a breaking of the solute-solute bonds, something which influence is particularly negligible for gases (endothermic);
3. Transfer of the CO_2 molecule from the gas to the liquid phase;
4. Reconnection of the solute-solute bonds in the absence of the CO_2 molecule, again negligible for gases (exothermic);
5. Creation of new solvent-solute bonds in the liquid phase (exothermic);
6. Reaction between the chemical binder, in this case MEA, and CO_2 (exothermic).

Regarding (1), the energy to break solvent-solvent bonds is strongly related to the enthalpy of vaporization of the solvent. In this particular case, all of the LVS have very similar enthalpy of vaporizations. Items

(2), (3) and (4) will naturally count the same for water-lean and aqueous solvents alike.

Item (5) is very special because it accounts for solvent-CO_2 interactions and for the release of energy associated with physical bonding through van der Waals forces. In a previous work [39], the heat of absorption of CO_2 in pure methanol, NMP and MEG was experimentally determined to be of respectively 15, 15 and 14 kJ/mol CO_2. Svensson et al. [11] obtained similar results for the heat of absorption in NMP and TEGDME. Additionally, these values are close to those calculated from solubility data through the van 't Hoff equation. There were found no experimental data for the enthalpy of absorption of CO_2 in pure water, but using the van 't Hoff equation, such can be estimated at about 20 kJ/mol CO_2. As one can see, the heat of absorption in physical absorbents does not appear to vary much from solvent to solvent.

Finally, item (6) is the one that counts the most overall, since the exothermicity of the MEA-CO_2 reactions surpasses by far the endothermicities of processes (1)-(2) and the exothermicity of processes (4)-(5). It is slightly affected by the stabilization provided by the solvent molecules surrounding the reactants, but mostly it is driven by the reaction alone, being quite similar for all solvents alike.

There follow two conclusions. The first one is that all heat of absorptions for similar solvents in which the chemical binder is the same should be similar. This is observed in Fig. 6. Furthermore, the heat of absorption for water-lean solvents made with good physical absorbents should at least be higher, not lower, than that of aqueous solvents. This is supported by the slightly higher heats of NMP + MEA 30 %w/w and sulfolane + MEA 30 %w/w measured in this work. Both these observations go against what is stated by Leites [26], who asserts that the enthalpy of absorption in water-lean solvents should be lower than that of aqueous solvents. This is true only in the very short span after $\alpha \approx 0.50$, where chemical reaction does not play the main role in CO_2 absorption anymore. However, for the interval that concerns most industrial purposes, where chemical binding is involved, the heat of absorption of water-lean solvents is similar if not higher than that of aqueous solvents with the same amine.

Despite this increase in enthalpy of absorption, there might be a way in which these LVS water-lean solvents could provide lower reboiler duties in an industrial scenario. To illustrate this, one needs to consider Eq. (1) needed for calculating the reboiler heat duty according to Oexmann and Kather [40].

$$Q^{reb} = \frac{C_{P,solv} \cdot \Delta T}{\Delta\alpha \cdot x} \cdot \frac{MM_{solv}}{MM_{CO2}} + \Delta H_{dil}^{vap} \cdot \frac{p_{dil}}{p_{CO2}} \cdot \frac{1}{MM_{CO2}} + \frac{\Delta H^{abs}}{MM_{CO2}} \quad (1)$$

In Eq. (1), the first term on the right-hand side refers to sensible heat needed for heating the solution up from the temperature it leaves the cross-heat exchanger up to the reboiler temperature, the second term refers to vaporization heat to boil solvent (mainly diluent, as most amines for industrial applications are ideally not volatile) at the reboiler temperature and produce stripping gas, and the third and final term refers to the heat of absorption itself. Table 3 shows data required for these calculations. The enthalpy of absorption shown is the average of the integral enthalpy of absorption obtained at 393 K in the interval referent to chemical binding. The $\Delta\alpha$ is the difference in loadings for $p_{CO2} \approx 1.0$ bar between 313 K and 393 K, such value of p_{CO2} being chosen merely as a common ground so that the total pressure in the stripper ($p_{CO2} + p_{dil}$) can be higher than 1.0 bar both for aqueous and non-aqueous solvents. The diluent partial pressure p_{dil} is the pressure measured in the course of the VLE experiments at 393 K for unloaded solutions. Both M_{solv} and $\times$ are properties of the unloaded solvent. Finally, the heat capacity of the mixed solvent (diluent + MEA) and the enthalpy of vaporization of the diluent alone were gathered from the literature [41], with C_p being estimated with a linear mixing rule.

Table 4
Results of the desorber heat duty calculations.

	H2O + MEA	MEG + MEA	NMP + MEA	THFA + MEA
Q^{sens} (MJ/kg CO_2)	0.12	0.21	0.35	0.24
Q^{vap} (MJ/kg CO_2)	1.66	0.23	0.22	0.27
Q^{abs} (MJ/kg CO_2)	1.93	2.16	2.16	2.16
Q^{reb} (MJ/kg CO_2)	3.71	2.60	2.72	2.67

With Eq. (1) and the parameters in Table 3, Table 4 can be derived. Though many approximations were made, it is remarkable that the energy consumption obtained for aqueous MEA 30 %w/w is very close to that of 3.7 MJ/kg reported by multiple studies [42–44]. This indicates the validity of these calculations at least for obtaining very preliminary results.

It can be clearly seen in Table 4 that, although the LVS analyzed present higher heat of absorption, they still offer competitive advantages when compared to regular aqueous solvents due to their very low heat of vaporization. This low heat of vaporization does not come from low enthalpies of vaporization, as can be observed in Table 4, but from the low vapor pressure of the diluent. In other words, whereas the LVS studied have a heat of absorption 12% higher than aqueous MEA, their heat of vaporization is still more than 80% lower. The heat of vaporization of aqueous MEA constitutes roughly 45% of its total desorber duty, being almost as important as the heat of absorption itself (52%). In Table 4 it also becomes evident that the $\Delta\alpha$ is greater for the water-lean solvents with NMP and THFA than for aqueous MEA 30 %w/w. This is a good indicator that regeneration of some novel absorbents may be facilitated by the way they benefit from temperature swings to desorb more CO_2, a phenomenon which was also observed by Rivas and Prausnitz [23] for NMP-based water-lean solvents.

In conclusion, the substitution of water for THFA could perhaps reduce the reboiler heat duty by 28%, the substitution for NMP could reduce it by 27% and that for MEG could reduce it by 30%. One might tentatively compare these energetic economies to those of respectively 33%, 33% and 13% obtained by Semenova and Leites [8], although that study presupposes different compositions and conditions than those employed in this research. It is also important to notice that these are all preliminary results that do not take into consideration factors as the viscosity of the liquids or their surface tension. Mass transfer is very dependent on these properties, and they strongly influence how close to equilibrium one can operate in the absorber. MEG + MEA 30 %w/w,

Table 3
Values used for desorber heat duty calculations.

	H2O + MEA	MEG + MEA	NMP + MEA	THFA + MEA
$C_{P,solv}$ (kJ/K.mol solv.)	0.08	0.15	0.34	0.18
MM_{solv} (kg/mol solv.)	0.031	0.062	0.088	0.102
$\Delta\alpha$ (mol CO_2/mol MEA)	0.28	0.27	0.38	0.34
x (mol MEA/mol solv.)	0.127	0.303	0.410	0.417
p_{dil} (bar)	1.80	0.16	0.19	0.25
ΔH_{dil}^{vap} (kJ/mol dil.)	40.5	61.1	49.5	46.5
ΔH^{abs} (kJ/mol CO_2)	85	95	95	95

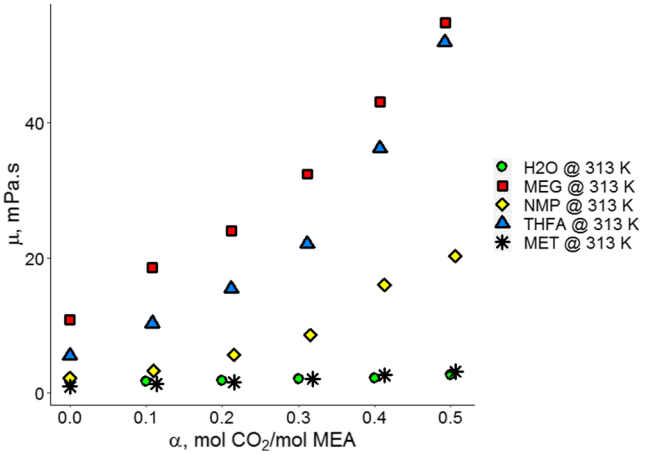

Fig. 11. Viscosities of the LVS and of methanol + MEA 30 %w/w under different loadings at 40 °C.

for example, presents a very low desorber heat duty according to Table 4, but its viscosity is high to the point of it becoming noticeable how difficult it was to reach equilibrium when running experiments with it in the calorimeter. Something that is also not clear in this analysis is whether desorption would be performed easily with such small vaporization of solvent. The formation of steam is important for stripping of CO_2 in the regeneration column. Thermodynamics and chemical equilibrium alone would possibly not be enough to assure the regeneration that is expected of these solvents in an industrial context.

The viscosities of both methanol + MEA 30 %w/w (scattered *) and several LVS (MEG = scattered □, NMP = scattered □, THFA = scattered △) with various CO_2 loadings were measured at 313 K and compared to that of aqueous MEA 30 %w/w (scattered ○) under similar conditions. The results are presented in Fig. 11. It can be clearly noticed that not only are the viscosities of the unloaded LVS higher than that of aqueous MEA 30 %w/w, they also increase more steeply with the addition of CO_2 to the medium. While the viscosity of aqueous MEA 30 %w/w increases roughly 10% for each extra 0.10 mol CO_2/mol MEA added, those of NMP + MEA 30 %w/w, THFA + MEA 30 %w/w and MEG + MEA 30 %w/w increase respectively 58%, 56% and 37%. Meanwhile, for methanol + MEA 30 %w/w, even if its initial viscosity is lower than that of aqueous MEA, each 0.10 mol CO_2/mol MEA brings about an increase of 26% in the measured viscosity. Because of this, and taking into account the Stokes-Einstein correlation between viscosity and diffusivity coefficient, it is to be expected that mass transfer in the water-lean solvent gets progressively difficult the more CO_2 is absorbed. This has been observed experimentally by Yuan and Rochelle [45] and again by Wanderley et al. [27].

3.6. Low- and non-aqueous water-lean solvents: THFA + H2O + MEA in different proportions

Throughout this work, VLE data was provided for non-aqueous water-lean solvents. By definition, however, a water-lean solvent can also contain a certain proportion of water, whose amount in comparison to that of the organic diluent certainly has an effect on VLE data. Therefore, the organic diluent THFA was chosen so that tests could be carried with varying proportions of water-diluent (0 %w/w, 20 %w/w, 50 %w/w, 80 %w/w, 100 %w/w) and, moreover, with different concentrations of MEA (10 %w/w, 20 %w/w, 30 %w/w) at the same

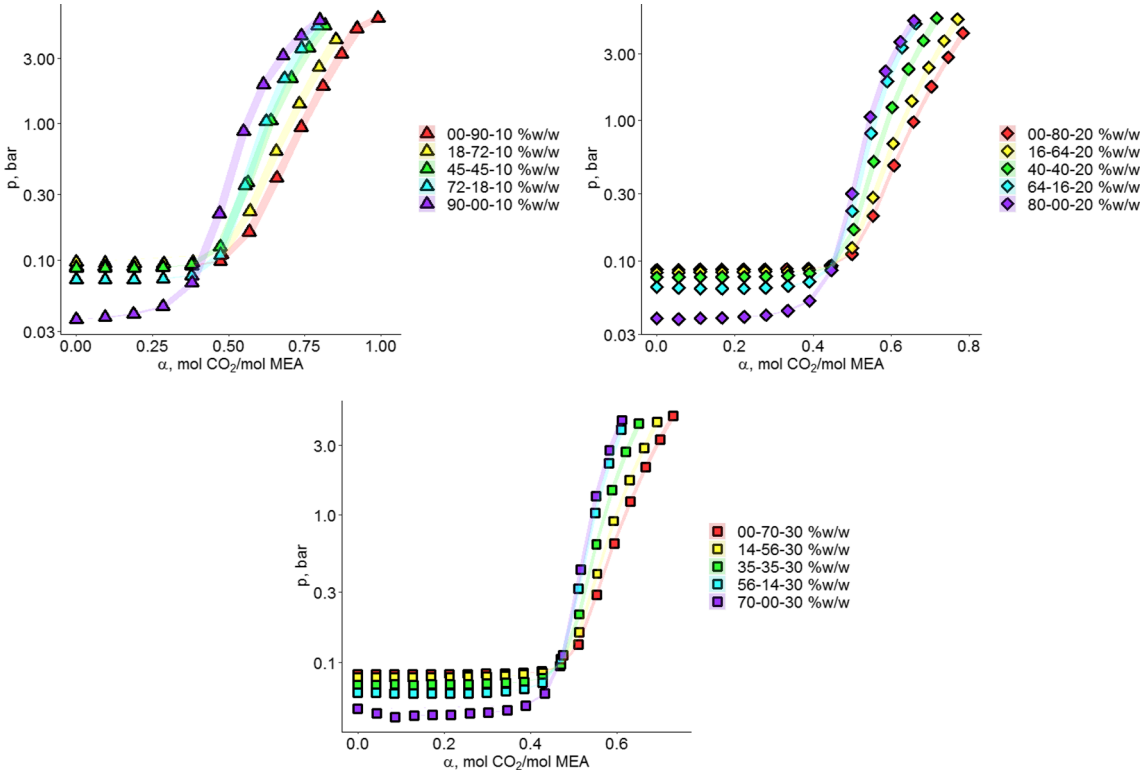

Fig. 12. Semilog plot of total pressure versus loading data for water-lean solvents with THFA, water and MEA in different proportions at 313 K, where the confidence interval for the calculated α is given by the horizontal span of the colored ribbons following the curves.

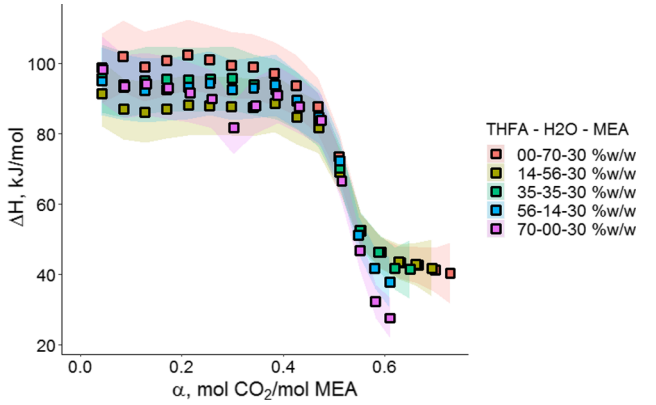

Fig. 13. Differential heat of absorption versus loading data for water-lean solvents containing THFA, water and MEA 30%w/w, where the confidence interval for the calculated ΔH is given by the vertical span of the colored ribbons following the curves.

temperature of 313 K. The results are shown in Fig. 12. These provide a very good example of the left-leaning shift mentioned previously in Wanderley et al. [27]: the addition of an organic diluent with lower dielectric permittivity than water shifts the vapor-liquid equilibrium of the chemical solvent by promoting a de-stabilization of the carbamate or, conversely, increasing the activities of all electrolytic species in solution.

In all cases analyzed, aqueous MEA has the highest capacity for CO_2 absorption and addition of THFA to the diluent steadily reduces this capacity. Furthermore, for a fixed diluent composition, the molar capacity for CO_2 absorption decreases from solvents with 10 %w/w to solvents with 30 %w/w (but not the mass capacity, as $\alpha = 0.50$ in a 30 %w/w MEA solution equals 108 g CO_2/kg solvent while in a 10 %w/w solution it equals 36 g CO_2/kg solvent). It is also evident that the effect of physical absorption after full stoichiometric loading, i.e. the slope of the VLE curve after $\alpha \approx 0.50$, is more accentuated the less MEA is present in the solution. Therefore, whereas one can start to observe a slight crossover with the 10 %w/w MEA water-lean solvents (particularly visible between 90% and 72%w/w THFA in the first part of Fig. 12), those are not noticeable for higher concentrations of MEA. A more thorough discussion of this is carried in Wanderley et al. [39].

Regarding the differential heat of absorption of all these various water-lean solvents, the overlap among the data obtained for all compositions added to the experimental uncertainties inherent to the measurements makes it virtually impossible to derive any conclusions regarding how they vary with water content. This confusion can be seen for example in Fig. 13. All that can be safely said is that withdraw of water from the system reduces the heat of absorption of near-to-fully loaded water-lean solvents ($\alpha \approx 0.50$). Besides that, little difference is observable.

4. Conclusion

In this work, VLE and heat of absorption data was obtained for various water-lean solvents containing MEA. In all of them, a reduction in CO_2 absorption capacity was observed upon substitution of water for an organic diluent. The heat of absorption remains quite similar given the uncertainties of the experiment, and a theoretical framework has been proposed to justify these results. The heat of absorption is chiefly defined by the heat of reaction, and water-lean solvents with equal chemical binders should have equally similar heat of absorption. Nevertheless, this does not mean that there are no opportunities for water-lean solvents to be competitive. Particularly for the LVS, the low-volatility of the solvents and consequent reduction of heat of evaporation duties offers many interesting prospects.

Furthermore, it was assessed that subtraction of water from the medium affects the VLE curves by progressively dragging them away from that of aqueous MEA, towards lower CO_2 absorption capacities. This is precisely the same result found in Wanderley et al. [27]. Meanwhile, the extended capacity for CO_2 absorption in water-lean solvents after full stoichiometric loading has been approached in Wanderley et al. [39] and is again observed in this work.

Lastly, this work has outlined some of the characteristics to be avoided in organic diluents for water-lean solvent formulation. Too low dielectric permittivities are undesirable and, quite probably, ester and ketone functions should be avoided altogether, since they seem more prone to react in basic media such as that provided by strong amines. The resulting reduction of the pool of possibilities may be helpful for guiding future research.

These results are constrained to water-lean solvents containing MEA, where carbamate formation is the main mechanism for CO_2 absorption. This happens particularly because MEA is a strong amine, and could possibly be subverted with different sorts of amines such as secondary and tertiary ones. The search for alternative reaction mechanisms is by no means exhausted through these findings. Additionally, the lack of volatility and speciation data in this work implies yet more room for research on water-lean solvents. Moreover, the suggestion that lower regeneration duties could be obtained by shifting to LVS remains to be tested experimentally in larger-scale experimental studies.

Funding

This research was funded by the Faculty of Natural Sciences of the Norwegian University of Science and Technology (NTNU).

Declaration of Competing Interest

The authors declare no conflict of interest.

Acknowledgement

We acknowledge Rune Rennemo (NTNU) for his invaluable assistance in training on the use of the calorimeter and understanding of its inner workings.

Appendix A. Experimental data

See Tables A1–A3.

Table A1
VLE and differential heat of absorption data for aqueous MEA.

Solvent	T (°C)	p (mbar)	α (mol CO_2/mol MEA)	ΔH (kJ/mol CO_2)
H2O + MEA 10 %w/w	40	90 ± 2		
H2O + MEA 10 %w/w	40	89 ± 2	0.09 ± 0.02	114 ± 16
H2O + MEA 10 %w/w	40	89 ± 2	0.19 ± 0.02	103 ± 14
H2O + MEA 10 %w/w	40	89 ± 2	0.28 ± 0.02	108 ± 14
H2O + MEA 10 %w/w	40	90 ± 2	0.38 ± 0.02	97 ± 13
H2O + MEA 10 %w/w	40	98 ± 2	0.47 ± 0.02	84 ± 11
H2O + MEA 10 %w/w	40	161 ± 2	0.57 ± 0.02	56 ± 7
H2O + MEA 10 %w/w	40	399 ± 2	0.66 ± 0.01	47 ± 6
H2O + MEA 10 %w/w	40	942 ± 2	0.74 ± 0.01	44 ± 7
H2O + MEA 10 %w/w	40	1879 ± 2	0.81 ± 0.02	40 ± 7
H2O + MEA 10 %w/w	40	3239 ± 2	0.87 ± 0.02	38 ± 10
H2O + MEA 10 %w/w	40	4969 ± 2	0.92 ± 0.02	36 ± 15
H2O + MEA 10 %w/w	40	5918 ± 2	0.99 ± 0.03	12 ± 4
H2O + MEA 20 %w/w	40	87 ± 2		
H2O + MEA 20 %w/w	40	86 ± 2	0.056 ± 0.005	104 ± 16
H2O + MEA 20 %w/w	40	87 ± 2	0.111 ± 0.005	95 ± 16
H2O + MEA 20 %w/w	40	87 ± 2	0.166 ± 0.005	92 ± 16
H2O + MEA 20 %w/w	40	87 ± 2	0.223 ± 0.005	90 ± 16
H2O + MEA 20 %w/w	40	87 ± 2	0.278 ± 0.005	90 ± 16
H2O + MEA 20 %w/w	40	87 ± 2	0.333 ± 0.005	93 ± 16
H2O + MEA 20 %w/w	40	88 ± 2	0.389 ± 0.005	87 ± 16
H2O + MEA 20 %w/w	40	92 ± 2	0.444 ± 0.005	84 ± 16
H2O + MEA 20 %w/w	40	112 ± 2	0.500 ± 0.005	73 ± 16
H2O + MEA 20 %w/w	40	210 ± 2	0.554 ± 0.005	57 ± 16
H2O + MEA 20 %w/w	40	479 ± 2	0.607 ± 0.005	45 ± 16
H2O + MEA 20 %w/w	40	976 ± 2	0.658 ± 0.005	41 ± 16
H2O + MEA 20 %w/w	40	1753 ± 2	0.704 ± 0.006	41 ± 16
H2O + MEA 20 %w/w	40	2833 ± 2	0.747 ± 0.007	39 ± 16
H2O + MEA 20 %w/w	40	4230 ± 2	0.785 ± 0.009	39 ± 18
H2O + MEA 30 %w/w	40	83 ± 2		
H2O + MEA 30 %w/w	40	83 ± 2	0.094 ± 0.005	90 ± 4
H2O + MEA 30 %w/w	40	83 ± 2	0.187 ± 0.005	87 ± 4
H2O + MEA 30 %w/w	40	84 ± 2	0.281 ± 0.005	86 ± 4
H2O + MEA 30 %w/w	40	85 ± 2	0.376 ± 0.005	86 ± 4
H2O + MEA 30 %w/w	40	95 ± 2	0.471 ± 0.005	82 ± 3
H2O + MEA 30 %w/w	40	360 ± 2	0.563 ± 0.004	59 ± 2
H2O + MEA 30 %w/w	40	1635 ± 2	0.648 ± 0.005	43 ± 2
H2O + MEA 30 %w/w	40	4284 ± 2	0.720 ± 0.006	41 ± 3
H2O + MEA 30 %w/w	80	448 ± 2		
H2O + MEA 30 %w/w	80	452 ± 2	0.043 ± 0.004	88 ± 8
H2O + MEA 30 %w/w	80	453 ± 2	0.086 ± 0.004	86 ± 8
H2O + MEA 30 %w/w	80	456 ± 2	0.130 ± 0.004	89 ± 8
H2O + MEA 30 %w/w	80	459 ± 2	0.173 ± 0.004	89 ± 8
H2O + MEA 30 %w/w	80	464 ± 2	0.216 ± 0.004	91 ± 8
H2O + MEA 30 %w/w	80	466 ± 2	0.259 ± 0.004	92 ± 8
H2O + MEA 30 %w/w	80	477 ± 2	0.302 ± 0.004	95 ± 9
H2O + MEA 30 %w/w	80	492 ± 2	0.345 ± 0.004	91 ± 8
H2O + MEA 30 %w/w	80	523 ± 2	0.388 ± 0.004	89 ± 8
H2O + MEA 30 %w/w	80	586 ± 2	0.431 ± 0.004	87 ± 8
H2O + MEA 30 %w/w	80	745 ± 2	0.472 ± 0.004	79 ± 7
H2O + MEA 30 %w/w	80	1159 ± 2	0.513 ± 0.004	67 ± 6
H2O + MEA 30 %w/w	80	2042 ± 2	0.549 ± 0.004	61 ± 7
H2O + MEA 30 %w/w	80	3491 ± 2	0.582 ± 0.005	59 ± 9
H2O + MEA 30 %w/w	80	5452 ± 2	0.610 ± 0.007	53 ± 12
H2O + MEA 30 %w/w	120	1801 ± 2		
H2O + MEA 30 %w/w	120	1811 ± 2	0.043 ± 0.005	75 ± 8
H2O + MEA 30 %w/w	120	1841 ± 2	0.085 ± 0.005	86 ± 9
H2O + MEA 30 %w/w	120	1875 ± 2	0.128 ± 0.005	74 ± 8
H2O + MEA 30 %w/w	120	1921 ± 2	0.171 ± 0.005	78 ± 8
H2O + MEA 30 %w/w	120	1985 ± 2	0.213 ± 0.005	77 ± 8
H2O + MEA 30 %w/w	120	2080 ± 2	0.255 ± 0.005	79 ± 9
H2O + MEA 30 %w/w	120	2227 ± 2	0.298 ± 0.005	87 ± 9
H2O + MEA 30 %w/w	120	2469 ± 2	0.339 ± 0.005	87 ± 10
H2O + MEA 30 %w/w	120	2881 ± 2	0.379 ± 0.005	92 ± 11

Table A2
VLE and differential heat of absorption data for non-aqueous solvents with MEA.

Solvent	T (°C)	p (mbar)	α (mol CO_2/mol MEA)	ΔH (kJ/mol CO_2)
MET + MEA 30 %w/w	20	125 ± 2		
MET + MEA 30 %w/w	20	126 ± 2	0.044 ± 0.004	86 ± 8
MET + MEA 30 %w/w	20	128 ± 2	0.087 ± 0.004	84 ± 8
MET + MEA 30 %w/w	20	130 ± 2	0.130 ± 0.004	82 ± 8
MET + MEA 30 %w/w	20	132 ± 2	0.173 ± 0.004	81 ± 8
MET + MEA 30 %w/w	20	133 ± 2	0.216 ± 0.004	81 ± 8
MET + MEA 30 %w/w	20	135 ± 2	0.259 ± 0.004	80 ± 7
MET + MEA 30 %w/w	20	137 ± 2	0.303 ± 0.004	79 ± 7
MET + MEA 30 %w/w	20	139 ± 2	0.346 ± 0.004	80 ± 7
MET + MEA 30 %w/w	20	142 ± 2	0.390 ± 0.004	78 ± 7
MET + MEA 30 %w/w	20	147 ± 2	0.433 ± 0.004	77 ± 7
MET + MEA 30 %w/w	20	159 ± 2	0.477 ± 0.004	70 ± 6
MET + MEA 30 %w/w	20	200 ± 2	0.520 ± 0.004	61 ± 5
MET + MEA 30 %w/w	20	311 ± 2	0.562 ± 0.004	51 ± 5
MET + MEA 30 %w/w	20	526 ± 2	0.604 ± 0.004	45 ± 4
MET + MEA 30 %w/w	20	854 ± 2	0.646 ± 0.004	41 ± 4
MET + MEA 30 %w/w	20	1298 ± 2	0.686 ± 0.004	38 ± 4
MET + MEA 30 %w/w	20	1856 ± 2	0.726 ± 0.004	35 ± 4
MET + MEA 30 %w/w	20	2514 ± 2	0.764 ± 0.005	33 ± 4
MET + MEA 30 %w/w	20	3265 ± 2	0.803 ± 0.006	31 ± 5
MET + MEA 30 %w/w	20	4085 ± 2	0.840 ± 0.007	29 ± 5
MET + MEA 30 %w/w	20	4972 ± 2	0.877 ± 0.008	27 ± 6
MET + MEA 30 %w/w	20	5909 ± 2	0.913 ± 0.009	26 ± 6
MET + MEA 30 %w/w	40	301 ± 2		
MET + MEA 30 %w/w	40	304 ± 2	0.043 ± 0.004	97 ± 9
MET + MEA 30 %w/w	40	308 ± 2	0.086 ± 0.004	90 ± 9
MET + MEA 30 %w/w	40	313 ± 2	0.130 ± 0.004	89 ± 8
MET + MEA 30 %w/w	40	317 ± 2	0.172 ± 0.004	89 ± 9
MET + MEA 30 %w/w	40	323 ± 2	0.216 ± 0.004	86 ± 8
MET + MEA 30 %w/w	40	328 ± 2	0.258 ± 0.004	88 ± 8
MET + MEA 30 %w/w	40	335 ± 2	0.302 ± 0.004	85 ± 8
MET + MEA 30 %w/w	40	345 ± 2	0.345 ± 0.004	85 ± 8
MET + MEA 30 %w/w	40	360 ± 2	0.388 ± 0.004	82 ± 7
MET + MEA 30 %w/w	40	391 ± 2	0.431 ± 0.004	78 ± 7
MET + MEA 30 %w/w	40	465 ± 2	0.474 ± 0.004	73 ± 7
MET + MEA 30 %w/w	40	647 ± 2	0.517 ± 0.004	63 ± 6
MET + MEA 30 %w/w	40	1005 ± 2	0.557 ± 0.004	54 ± 5
MET + MEA 30 %w/w	40	1565 ± 2	0.596 ± 0.004	46 ± 5
MET + MEA 30 %w/w	40	2306 ± 2	0.634 ± 0.005	40 ± 5
MET + MEA 30 %w/w	40	3192 ± 2	0.671 ± 0.006	36 ± 5
MET + MEA 30 %w/w	40	4208 ± 2	0.706 ± 0.007	33 ± 6
MET + MEA 30 %w/w	40	5329 ± 2	0.741 ± 0.008	35 ± 8
MET + MEA 30 %w/w	40	6530 ± 2	0.775 ± 0.009	29 ± 7
MET + MEA 30 %w/w	80	1464 ± 2		
MET + MEA 30 %w/w	80	1489 ± 2	0.043 ± 0.005	89 ± 8
MET + MEA 30 %w/w	80	1520 ± 2	0.086 ± 0.005	98 ± 10
MET + MEA 30 %w/w	80	1559 ± 2	0.129 ± 0.005	96 ± 10
MET + MEA 30 %w/w	80	1606 ± 2	0.172 ± 0.005	97 ± 10
MET + MEA 30 %w/w	80	1667 ± 2	0.215 ± 0.005	95 ± 10
MET + MEA 30 %w/w	80	1750 ± 2	0.257 ± 0.005	93 ± 10
MET + MEA 30 %w/w	80	1869 ± 2	0.300 ± 0.005	89 ± 9
MET + MEA 30 %w/w	80	2048 ± 2	0.342 ± 0.005	87 ± 9
MET + MEA 30 %w/w	80	2331 ± 2	0.383 ± 0.005	82 ± 9
MET + MEA 30 %w/w	80	2776 ± 2	0.424 ± 0.005	77 ± 9
MET + MEA 30 %w/w	80	3456 ± 2	0.463 ± 0.005	69 ± 9
MET + MEA 30 %w/w	80	4412 ± 2	0.500 ± 0.006	61 ± 10
MET + MEA 30 %w/w	80	5640 ± 2	0.535 ± 0.007	54 ± 10
MET + MEA 30 %w/w	80	6998 ± 2	0.566 ± 0.008	48 ± 12
ACE + MEA 30 %w/w	20	189 ± 2		
ACE + MEA 30 %w/w	20	188 ± 2	0.047 ± 0.004	98 ± 9
ACE + MEA 30 %w/w	20	203 ± 2	0.085 ± 0.004	85 ± 9
ACE + MEA 30 %w/w	20	198 ± 2	0.128 ± 0.004	66 ± 6
ACE + MEA 30 %w/w	20	206 ± 2	0.170 ± 0.004	57 ± 6
ACE + MEA 30 %w/w	20	200 ± 2	0.219 ± 0.004	40 ± 3
ACE + MEA 30 %w/w	20	219 ± 2	0.255 ± 0.004	59 ± 7
ACE + MEA 30 %w/w	20	234 ± 2	0.298 ± 0.004	49 ± 5
ACE + MEA 30 %w/w	20	265 ± 2	0.340 ± 0.004	51 ± 5
ACE + MEA 30 %w/w	20	319 ± 2	0.382 ± 0.004	49 ± 5
ACE + MEA 30 %w/w	20	419 ± 2	0.424 ± 0.004	43 ± 4
ACE + MEA 30 %w/w	20	603 ± 2	0.466 ± 0.004	34 ± 3
ACE + MEA 30 %w/w	20	887 ± 2	0.507 ± 0.004	29 ± 3
ACE + MEA 30 %w/w	20	1287 ± 2	0.547 ± 0.004	26 ± 3
ACE + MEA 30 %w/w	20	1779 ± 2	0.586 ± 0.004	23 ± 3
ACE + MEA 30 %w/w	20	2339 ± 2	0.625 ± 0.005	20 ± 2

(*continued on next page*)

Table A2 (*continued*)

Solvent	T (°C)	p (mbar)	α (mol CO_2/mol MEA)	ΔH (kJ/mol CO_2)
ACE + MEA 30 %w/w	20	2952 ± 2	0.663 ± 0.005	19 ± 3
ACE + MEA 30 %w/w	20	3601 ± 2	0.701 ± 0.006	19 ± 3
ACE + MEA 30 %w/w	20	4276 ± 2	0.739 ± 0.007	18 ± 3
ACE + MEA 30 %w/w	20	4970 ± 2	0.778 ± 0.007	14 ± 3
MEG + MEA 30 %w/w	40	35 ± 2		
MEG + MEA 30 %w/w	40	35 ± 2	0.043 ± 0.004	92 ± 9
MEG + MEA 30 %w/w	40	34 ± 2	0.086 ± 0.004	87 ± 8
MEG + MEA 30 %w/w	40	34 ± 2	0.130 ± 0.004	85 ± 8
MEG + MEA 30 %w/w	40	33 ± 2	0.173 ± 0.004	87 ± 8
MEG + MEA 30 %w/w	40	33 ± 2	0.216 ± 0.004	80 ± 7
MEG + MEA 30 %w/w	40	33 ± 2	0.258 ± 0.004	86 ± 8
MEG + MEA 30 %w/w	40	34 ± 2	0.302 ± 0.004	86 ± 8
MEG + MEA 30 %w/w	40	35 ± 2	0.345 ± 0.004	85 ± 8
MEG + MEA 30 %w/w	40	37 ± 2	0.388 ± 0.004	85 ± 8
MEG + MEA 30 %w/w	40	45 ± 2	0.431 ± 0.004	84 ± 7
MEG + MEA 30 %w/w	40	80 ± 2	0.474 ± 0.004	81 ± 7
MEG + MEA 30 %w/w	40	271 ± 2	0.515 ± 0.004	70 ± 6
MEG + MEA 30 %w/w	40	894 ± 2	0.553 ± 0.004	49 ± 5
MEG + MEA 30 %w/w	40	2024 ± 2	0.586 ± 0.004	41 ± 5
MEG + MEA 30 %w/w	40	3575 ± 2	0.615 ± 0.005	38 ± 7
MEG + MEA 30 %w/w	40	5440 ± 2	0.641 ± 0.007	34 ± 9
MEG + MEA 30 %w/w	80	45 ± 2		
MEG + MEA 30 %w/w	80	47 ± 2	0.044 ± 0.004	101 ± 9
MEG + MEA 30 %w/w	80	50 ± 2	0.087 ± 0.004	98 ± 9
MEG + MEA 30 %w/w	80	53 ± 2	0.130 ± 0.004	97 ± 9
MEG + MEA 30 %w/w	80	59 ± 2	0.174 ± 0.004	95 ± 9
MEG + MEA 30 %w/w	80	69 ± 2	0.217 ± 0.004	95 ± 9
MEG + MEA 30 %w/w	80	84 ± 2	0.260 ± 0.004	93 ± 8
MEG + MEA 30 %w/w	80	112 ± 2	0.303 ± 0.004	93 ± 8
MEG + MEA 30 %w/w	80	163 ± 2	0.345 ± 0.004	92 ± 8
MEG + MEA 30 %w/w	80	272 ± 2	0.387 ± 0.004	90 ± 8
MEG + MEA 30 %w/w	80	521 ± 2	0.428 ± 0.004	88 ± 8
MEG + MEA 30 %w/w	80	1093 ± 2	0.467 ± 0.004	81 ± 8
MEG + MEA 30 %w/w	80	2285 ± 2	0.500 ± 0.004	71 ± 9
MEG + MEA 30 %w/w	80	4193 ± 2	0.528 ± 0.005	65 ± 12
MEG + MEA 30 %w/w	80	6606 ± 2	0.551 ± 0.008	57 ± 18
MEG + MEA 30 %w/w	120	164 ± 2		
MEG + MEA 30 %w/w	120	197 ± 2	0.041 ± 0.004	92 ± 9
MEG + MEA 30 %w/w	120	252 ± 2	0.083 ± 0.004	99 ± 9
MEG + MEA 30 %w/w	120	331 ± 2	0.124 ± 0.004	97 ± 9
MEG + MEA 30 %w/w	120	446 ± 2	0.164 ± 0.004	95 ± 9
MEG + MEA 30 %w/w	120	616 ± 2	0.204 ± 0.004	93 ± 9
MEG + MEA 30 %w/w	120	871 ± 2	0.244 ± 0.004	93 ± 9
MEG + MEA 30 %w/w	120	1260 ± 2	0.282 ± 0.004	92 ± 9
MEG + MEA 30 %w/w	120	1854 ± 2	0.320 ± 0.004	95 ± 10
MEG + MEA 30 %w/w	120	2759 ± 2	0.355 ± 0.005	93 ± 11
MEG + MEA 30 %w/w	120	4082 ± 2	0.388 ± 0.005	90 ± 14
MEG + MEA 30 %w/w	120	5924 ± 2	0.417 ± 0.006	85 ± 17
NMP + MEA 30 %w/w	40	30 ± 2		
NMP + MEA 30 %w/w	40	30 ± 2	0.043 ± 0.004	106 ± 10
NMP + MEA 30 %w/w	40	30 ± 2	0.085 ± 0.004	105 ± 10
NMP + MEA 30 %w/w	40	29 ± 2	0.128 ± 0.004	105 ± 10
NMP + MEA 30 %w/w	40	29 ± 2	0.170 ± 0.004	104 ± 10
NMP + MEA 30 %w/w	40	30 ± 2	0.212 ± 0.004	103 ± 10
NMP + MEA 30 %w/w	40	30 ± 2	0.255 ± 0.004	102 ± 9
NMP + MEA 30 %w/w	40	30 ± 2	0.297 ± 0.004	101 ± 9
NMP + MEA 30 %w/w	40	31 ± 2	0.340 ± 0.004	99 ± 9
NMP + MEA 30 %w/w	40	32 ± 2	0.382 ± 0.004	96 ± 9
NMP + MEA 30 %w/w	40	35 ± 2	0.425 ± 0.004	94 ± 8
NMP + MEA 30 %w/w	40	45 ± 2	0.467 ± 0.004	88 ± 8
NMP + MEA 30 %w/w	40	90 ± 2	0.509 ± 0.004	77 ± 8
NMP + MEA 30 %w/w	40	257 ± 2	0.550 ± 0.004	59 ± 6
NMP + MEA 30 %w/w	40	693 ± 2	0.589 ± 0.004	48 ± 5
NMP + MEA 30 %w/w	40	1478 ± 2	0.625 ± 0.004	40 ± 5
NMP + MEA 30 %w/w	40	2578 ± 2	0.658 ± 0.005	34 ± 5
NMP + MEA 30 %w/w	40	3992 ± 2	0.689 ± 0.006	30 ± 6
NMP + MEA 30 %w/w	40	5430 ± 2	0.719 ± 0.007	28 ± 7
NMP + MEA 30 %w/w	80	60 ± 2		
NMP + MEA 30 %w/w	80	64 ± 2	0.042 ± 0.004	102 ± 10
NMP + MEA 30 %w/w	80	67 ± 2	0.086 ± 0.004	100 ± 9
NMP + MEA 30 %w/w	80	76 ± 2	0.128 ± 0.004	105 ± 10
NMP + MEA 30 %w/w	80	83 ± 2	0.171 ± 0.004	110 ± 10
NMP + MEA 30 %w/w	80	91 ± 2	0.215 ± 0.004	105 ± 10
NMP + MEA 30 %w/w	80	105 ± 2	0.258 ± 0.004	104 ± 9
NMP + MEA 30 %w/w	80	126 ± 2	0.301 ± 0.004	102 ± 9

(*continued on next page*)

Table A2 (*continued*)

Solvent	T (°C)	p (mbar)	α (mol CO_2/mol MEA)	ΔH (kJ/mol CO_2)
NMP + MEA 30 %w/w	80	163 ± 2	0.344 ± 0.004	100 ± 9
NMP + MEA 30 %w/w	80	231 ± 2	0.387 ± 0.004	97 ± 9
NMP + MEA 30 %w/w	80	365 ± 2	0.428 ± 0.004	93 ± 8
NMP + MEA 30 %w/w	80	638 ± 2	0.469 ± 0.004	86 ± 8
NMP + MEA 30 %w/w	80	1167 ± 2	0.508 ± 0.004	76 ± 7
NMP + MEA 30 %w/w	80	2089 ± 2	0.544 ± 0.004	64 ± 7
NMP + MEA 30 %w/w	80	3447 ± 2	0.577 ± 0.005	54 ± 8
NMP + MEA 30 %w/w	80	5178 ± 2	0.607 ± 0.006	46 ± 9
NMP + MEA 30 %w/w	120	193 ± 2		
NMP + MEA 30 %w/w	120	335 ± 2	0.042 ± 0.004	95 ± 9
NMP + MEA 30 %w/w	120	464 ± 2	0.084 ± 0.004	90 ± 9
NMP + MEA 30 %w/w	120	608 ± 2	0.126 ± 0.004	93 ± 9
NMP + MEA 30 %w/w	120	784 ± 2	0.169 ± 0.004	94 ± 9
NMP + MEA 30 %w/w	120	1012 ± 2	0.210 ± 0.004	99 ± 9
NMP + MEA 30 %w/w	120	1317 ± 2	0.252 ± 0.004	97 ± 9
NMP + MEA 30 %w/w	120	1723 ± 2	0.291 ± 0.004	99 ± 10
NMP + MEA 30 %w/w	120	2287 ± 2	0.331 ± 0.005	95 ± 10
NMP + MEA 30 %w/w	120	3055 ± 2	0.369 ± 0.005	92 ± 11
NMP + MEA 30 %w/w	120	4072 ± 2	0.404 ± 0.005	87 ± 13
NMP + MEA 30 %w/w	120	5391 ± 2	0.438 ± 0.006	82 ± 14
NMP + MEA 30 %w/w	120	7003 ± 2	0.469 ± 0.008	76 ± 18
THFA + MEA 10 %w/w	40	37 ± 2		
THFA + MEA 10 %w/w	40	38 ± 2	0.09 ± 0.02	99 ± 13
THFA + MEA 10 %w/w	40	40 ± 2	0.19 ± 0.02	99 ± 13
THFA + MEA 10 %w/w	40	46 ± 2	0.28 ± 0.02	94 ± 12
THFA + MEA 10 %w/w	40	68 ± 2	0.38 ± 0.01	93 ± 12
THFA + MEA 10 %w/w	40	219 ± 2	0.47 ± 0.01	85 ± 11
THFA + MEA 10 %w/w	40	877 ± 2	0.55 ± 0.01	52 ± 8
THFA + MEA 10 %w/w	40	1936 ± 2	0.61 ± 0.01	33 ± 7
THFA + MEA 10 %w/w	40	3140 ± 2	0.68 ± 0.02	26 ± 6
THFA + MEA 10 %w/w	40	4419 ± 2	0.74 ± 0.02	23 ± 7
THFA + MEA 10 %w/w	40	5731 ± 2	0.80 ± 0.02	21 ± 8
THFA + MEA 20 %w/w	40	39 ± 2		
THFA + MEA 20 %w/w	40	38 ± 2	0.056 ± 0.007	97 ± 11
THFA + MEA 20 %w/w	40	39 ± 2	0.112 ± 0.007	94 ± 11
THFA + MEA 20 %w/w	40	39 ± 2	0.167 ± 0.007	95 ± 11
THFA + MEA 20 %w/w	40	40 ± 2	0.224 ± 0.007	92 ± 10
THFA + MEA 20 %w/w	40	41 ± 2	0.280 ± 0.007	92 ± 10
THFA + MEA 20 %w/w	40	44 ± 2	0.336 ± 0.007	92 ± 10
THFA + MEA 20 %w/w	40	52 ± 2	0.392 ± 0.007	89 ± 10
THFA + MEA 20 %w/w	40	86 ± 2	0.448 ± 0.007	87 ± 9
THFA + MEA 20 %w/w	40	301 ± 2	0.501 ± 0.006	73 ± 8
THFA + MEA 20 %w/w	40	1063 ± 2	0.547 ± 0.006	49 ± 6
THFA + MEA 20 %w/w	40	2251 ± 2	0.587 ± 0.007	34 ± 6
THFA + MEA 20 %w/w	40	3657 ± 2	0.624 ± 0.009	29 ± 6
THFA + MEA 20 %w/w	40	5182 ± 2	0.66 ± 0.01	26 ± 8
THFA + MEA 30 %w/w	40	48 ± 2		
THFA + MEA 30 %w/w	40	45 ± 2	0.044 ± 0.004	98 ± 9
THFA + MEA 30 %w/w	40	43 ± 2	0.086 ± 0.004	93 ± 9
THFA + MEA 30 %w/w	40	43 ± 2	0.130 ± 0.004	94 ± 9
THFA + MEA 30 %w/w	40	44 ± 2	0.173 ± 0.004	93 ± 9
THFA + MEA 30 %w/w	40	44 ± 2	0.216 ± 0.004	92 ± 9
THFA + MEA 30 %w/w	40	45 ± 2	0.259 ± 0.004	90 ± 8
THFA + MEA 30 %w/w	40	45 ± 2	0.302 ± 0.004	82 ± 7
THFA + MEA 30 %w/w	40	47 ± 2	0.345 ± 0.004	88 ± 8
THFA + MEA 30 %w/w	40	51 ± 2	0.389 ± 0.004	91 ± 8
THFA + MEA 30 %w/w	40	61 ± 2	0.432 ± 0.004	88 ± 8
THFA + MEA 30 %w/w	40	112 ± 2	0.475 ± 0.004	84 ± 7
THFA + MEA 30 %w/w	40	426 ± 2	0.515 ± 0.004	67 ± 6
THFA + MEA 30 %w/w	40	1354 ± 2	0.551 ± 0.004	47 ± 5
THFA + MEA 30 %w/w	40	2754 ± 2	0.582 ± 0.005	32 ± 5
THFA + MEA 30 %w/w	40	4435 ± 2	0.610 ± 0.006	28 ± 6
THFA + MEA 30 %w/w	80	79 ± 2		
THFA + MEA 30 %w/w	80	83 ± 2	0.044 ± 0.004	97 ± 9
THFA + MEA 30 %w/w	80	88 ± 2	0.087 ± 0.004	97 ± 9
THFA + MEA 30 %w/w	80	95 ± 2	0.131 ± 0.004	97 ± 9
THFA + MEA 30 %w/w	80	105 ± 2	0.174 ± 0.004	97 ± 9
THFA + MEA 30 %w/w	80	121 ± 2	0.218 ± 0.004	97 ± 9
THFA + MEA 30 %w/w	80	144 ± 2	0.261 ± 0.004	96 ± 9
THFA + MEA 30 %w/w	80	184 ± 2	0.304 ± 0.004	94 ± 8
THFA + MEA 30 %w/w	80	258 ± 2	0.347 ± 0.004	90 ± 8
THFA + MEA 30 %w/w	80	408 ± 2	0.389 ± 0.004	87 ± 8
THFA + MEA 30 %w/w	80	739 ± 2	0.430 ± 0.004	84 ± 8
THFA + MEA 30 %w/w	80	1468 ± 2	0.468 ± 0.004	80 ± 8
THFA + MEA 30 %w/w	80	2793 ± 2	0.501 ± 0.005	67 ± 9

(*continued on next page*)

Table A2 (*continued*)

Solvent	T (°C)	p (mbar)	α (mol CO_2/mol MEA)	ΔH (kJ/mol CO_2)
THFA + MEA 30 %w/w	80	4692 ± 2	0.529 ± 0.006	54 ± 11
THFA + MEA 30 %w/w	120	253 ± 2		
THFA + MEA 30 %w/w	120	387 ± 2	0.040 ± 0.004	90 ± 9
THFA + MEA 30 %w/w	120	531 ± 2	0.081 ± 0.004	92 ± 9
THFA + MEA 30 %w/w	120	703 ± 2	0.121 ± 0.004	92 ± 9
THFA + MEA 30 %w/w	120	924 ± 2	0.162 ± 0.004	93 ± 9
THFA + MEA 30 %w/w	120	1221 ± 2	0.201 ± 0.004	95 ± 9
THFA + MEA 30 %w/w	120	1628 ± 2	0.240 ± 0.004	99 ± 10
THFA + MEA 30 %w/w	120	2195 ± 2	0.278 ± 0.004	99 ± 11
THFA + MEA 30 %w/w	120	2983 ± 2	0.314 ± 0.004	94 ± 11
THFA + MEA 30 %w/w	120	4063 ± 2	0.349 ± 0.005	90 ± 13
THFA + MEA 30 %w/w	120	5494 ± 2	0.381 ± 0.006	84 ± 15
THFA + MEA 30 %w/w	120	7300 ± 2	0.411 ± 0.008	77 ± 18
SULF + MEA 30 %w/w	40	29 ± 2		
SULF + MEA 30 %w/w	40	28 ± 2	0.043 ± 0.004	100 ± 10
SULF + MEA 30 %w/w	40	28 ± 2	0.086 ± 0.004	98 ± 9
SULF + MEA 30 %w/w	40	28 ± 2	0.129 ± 0.004	101 ± 10
SULF + MEA 30 %w/w	40	28 ± 2	0.172 ± 0.004	105 ± 10
SULF + MEA 30 %w/w	40	28 ± 2	0.215 ± 0.004	103 ± 10
SULF + MEA 30 %w/w	40	28 ± 2	0.258 ± 0.004	101 ± 9
SULF + MEA 30 %w/w	40	28 ± 2	0.301 ± 0.004	98 ± 9
SULF + MEA 30 %w/w	40	28 ± 2	0.344 ± 0.004	97 ± 9
SULF + MEA 30 %w/w	40	29 ± 2	0.387 ± 0.004	95 ± 8
SULF + MEA 30 %w/w	40	30 ± 2	0.430 ± 0.004	95 ± 8
SULF + MEA 30 %w/w	40	46 ± 2	0.474 ± 0.004	92 ± 8
SULF + MEA 30 %w/w	40	312 ± 2	0.514 ± 0.004	72 ± 7
SULF + MEA 30 %w/w	40	1330 ± 2	0.547 ± 0.004	38 ± 4
SULF + MEA 30 %w/w	40	2752 ± 2	0.576 ± 0.005	29 ± 4
SULF + MEA 30 %w/w	40	4369 ± 2	0.604 ± 0.006	25 ± 6
SULF + MEA 30 %w/w	40	6059 ± 2	0.630 ± 0.008	23 ± 7
CC5 + MEA 30 %w/w	40	71 ± 2		
CC5 + MEA 30 %w/w	40	74 ± 2	0.042 ± 0.004	82 ± 8
CC5 + MEA 30 %w/w	40	75 ± 2	0.085 ± 0.004	66 ± 6
CC5 + MEA 30 %w/w	40	76 ± 2	0.128 ± 0.004	63 ± 6
CC5 + MEA 30 %w/w	40	79 ± 2	0.170 ± 0.004	64 ± 6
CC5 + MEA 30 %w/w	40	85 ± 2	0.213 ± 0.004	62 ± 6
CC5 + MEA 30 %w/w	40	99 ± 2	0.256 ± 0.004	60 ± 6
CC5 + MEA 30 %w/w	40	132 ± 2	0.299 ± 0.004	59 ± 5
CC5 + MEA 30 %w/w	40	167 ± 2	0.341 ± 0.004	57 ± 5
CC5 + MEA 30 %w/w	40	218 ± 2	0.384 ± 0.004	56 ± 5
CC5 + MEA 30 %w/w	40	295 ± 2	0.427 ± 0.004	56 ± 5
CC5 + MEA 30 %w/w	40	485 ± 2	0.468 ± 0.004	57 ± 5
CC5 + MEA 30 %w/w	40	936 ± 2	0.507 ± 0.004	47 ± 5
CC5 + MEA 30 %w/w	40	1807 ± 2	0.544 ± 0.004	42 ± 5
CC5 + MEA 30 %w/w	80	377 ± 2		
CC5 + MEA 30 %w/w	80	337 ± 2	0.042 ± 0.005	188 ± 20
CC5 + MEA 30 %w/w	80	318 ± 2	0.084 ± 0.005	100 ± 10
CC5 + MEA 30 %w/w	80	306 ± 2	0.127 ± 0.005	96 ± 10
CC5 + MEA 30 %w/w	80	299 ± 2	0.169 ± 0.004	97 ± 10
CC5 + MEA 30 %w/w	80	297 ± 2	0.211 ± 0.004	86 ± 8
CC5 + MEA 30 %w/w	80	301 ± 2	0.254 ± 0.004	92 ± 9
CC5 + MEA 30 %w/w	80	313 ± 2	0.297 ± 0.004	86 ± 8
CC5 + MEA 30 %w/w	80	338 ± 2	0.339 ± 0.004	70 ± 7
CC5 + MEA 30 %w/w	80	420 ± 2	0.381 ± 0.004	87 ± 8
CC5 + MEA 30 %w/w	80	628 ± 2	0.423 ± 0.004	85 ± 8
CC5 + MEA 30 %w/w	80	1189 ± 2	0.462 ± 0.004	71 ± 7
CC5 + MEA 30 %w/w	80	2407 ± 2	0.496 ± 0.005	58 ± 7
CC5 + MEA 30 %w/w	80	4259 ± 2	0.525 ± 0.006	45 ± 8
CC5 + MEA 30 %w/w	80	6498 ± 2	0.551 ± 0.008	43 ± 12
CC5 + MEA 30 %w/w	120	1411 ± 2		
CC5 + MEA 30 %w/w	120	1480 ± 2	0.033 ± 0.005	157 ± 22
CC5 + MEA 30 %w/w	120	1527 ± 2	0.066 ± 0.005	112 ± 15
CC5 + MEA 30 %w/w	120	1606 ± 2	0.099 ± 0.005	123 ± 17
CC5 + MEA 30 %w/w	120	1646 ± 2	0.132 ± 0.005	102 ± 14
CC5 + MEA 30 %w/w	120	1692 ± 2	0.165 ± 0.005	100 ± 14
CC5 + MEA 30 %w/w	120	1772 ± 2	0.198 ± 0.005	106 ± 15
CC5 + MEA 30 %w/w	120	1901 ± 2	0.230 ± 0.005	96 ± 13
CC5 + MEA 30 %w/w	120	2083 ± 2	0.262 ± 0.005	86 ± 12
CC5 + MEA 30 %w/w	120	2389 ± 2	0.294 ± 0.005	87 ± 13
CC5 + MEA 30 %w/w	120	2896 ± 2	0.324 ± 0.005	85 ± 13
CC5 + MEA 30 %w/w	120	3664 ± 2	0.352 ± 0.005	87 ± 16
CC5 + MEA 30 %w/w	120	4733 ± 2	0.379 ± 0.006	79 ± 17
CC5 + MEA 30 %w/w	120	4700 ± 2	0.412 ± 0.006	52 ± 9
CC5 + MEA 30 %w/w	120	5006 ± 2	0.444 ± 0.007	45 ± 8
FA + MEA 30 %w/w	40	21 ± 2		

(*continued on next page*)

Table A2 (*continued*)

Solvent	T (°C)	p (mbar)	α (mol CO_2/mol MEA)	ΔH (kJ/mol CO_2)
FA + MEA 30 %w/w	40	22 ± 2	0.018 ± 0.002	94 ± 9
FA + MEA 30 %w/w	40	22 ± 2	0.036 ± 0.002	91 ± 9
FA + MEA 30 %w/w	40	23 ± 2	0.055 ± 0.002	88 ± 9
FA + MEA 30 %w/w	40	24 ± 2	0.073 ± 0.002	89 ± 9
FA + MEA 30 %w/w	40	25 ± 2	0.091 ± 0.002	87 ± 8
FA + MEA 30 %w/w	40	25 ± 2	0.109 ± 0.002	87 ± 8
FA + MEA 30 %w/w	40	27 ± 2	0.128 ± 0.002	87 ± 8
FA + MEA 30 %w/w	40	31 ± 2	0.146 ± 0.002	86 ± 8
FA + MEA 30 %w/w	40	41 ± 2	0.164 ± 0.002	84 ± 8
FA + MEA 30 %w/w	40	71 ± 2	0.183 ± 0.002	83 ± 7
FA + MEA 30 %w/w	40	196 ± 2	0.201 ± 0.002	78 ± 7
FA + MEA 30 %w/w	40	739 ± 2	0.217 ± 0.002	63 ± 6
FA + MEA 30 %w/w	40	1948 ± 2	0.231 ± 0.002	45 ± 6
FA + MEA 30 %w/w	40	3606 ± 2	0.243 ± 0.002	35 ± 6
FA + MEA 30 %w/w	40	5443 ± 2	0.252 ± 0.003	36 ± 12
FA + MEA 30 %w/w	80	62 ± 2		
FA + MEA 30 %w/w	80	73 ± 2	0.018 ± 0.002	95 ± 9
FA + MEA 30 %w/w	80	85 ± 2	0.036 ± 0.002	93 ± 9
FA + MEA 30 %w/w	80	99 ± 2	0.054 ± 0.002	91 ± 9
FA + MEA 30 %w/w	80	118 ± 2	0.072 ± 0.002	91 ± 9
FA + MEA 30 %w/w	80	149 ± 2	0.090 ± 0.002	90 ± 8
FA + MEA 30 %w/w	80	197 ± 2	0.108 ± 0.002	87 ± 8
FA + MEA 30 %w/w	80	278 ± 2	0.126 ± 0.002	85 ± 8
FA + MEA 30 %w/w	80	422 ± 2	0.144 ± 0.002	83 ± 8
FA + MEA 30 %w/w	80	699 ± 2	0.161 ± 0.002	84 ± 8
FA + MEA 30 %w/w	80	1240 ± 2	0.178 ± 0.002	83 ± 8
FA + MEA 30 %w/w	80	2242 ± 2	0.193 ± 0.002	76 ± 9
FA + MEA 30 %w/w	80	3800 ± 2	0.206 ± 0.002	63 ± 10
FA + MEA 30 %w/w	80	5873 ± 2	0.217 ± 0.002	55 ± 14

Table A3
VLE and differential heat of absorption data for low-aqueous solvents with THFA and MEA.

THFA : H2O : MEA	T (°C)	p (mbar)	α (mol CO_2/mol MEA)	ΔH (kJ/mol CO_2)
18 : 72 : 10 (%w/w)	40	96 ± 2		
18 : 72 : 10 (%w/w)	40	95 ± 2	0.09 ± 0.02	92 ± 12
18 : 72 : 10 (%w/w)	40	94 ± 2	0.19 ± 0.02	90 ± 11
18 : 72 : 10 (%w/w)	40	94 ± 2	0.29 ± 0.01	90 ± 11
18 : 72 : 10 (%w/w)	40	96 ± 2	0.38 ± 0.01	87 ± 11
18 : 72 : 10 (%w/w)	40	110 ± 2	0.48 ± 0.01	79 ± 10
18 : 72 : 10 (%w/w)	40	228 ± 2	0.57 ± 0.01	58 ± 7
18 : 72 : 10 (%w/w)	40	625 ± 2	0.66 ± 0.01	45 ± 6
18 : 72 : 10 (%w/w)	40	1395 ± 2	0.73 ± 0.01	40 ± 6
18 : 72 : 10 (%w/w)	40	2586 ± 2	0.80 ± 0.02	40 ± 9
18 : 72 : 10 (%w/w)	40	4135 ± 2	0.85 ± 0.02	37 ± 12
45 : 45 : 10 (%w/w)	40	88 ± 2		
45 : 45 : 10 (%w/w)	40	88 ± 2	0.09 ± 0.02	92 ± 13
45 : 45 : 10 (%w/w)	40	88 ± 2	0.19 ± 0.02	90 ± 12
45 : 45 : 10 (%w/w)	40	88 ± 2	0.28 ± 0.02	90 ± 12
45 : 45 : 10 (%w/w)	40	93 ± 2	0.38 ± 0.02	88 ± 12
45 : 45 : 10 (%w/w)	40	125 ± 2	0.47 ± 0.02	81 ± 11
45 : 45 : 10 (%w/w)	40	369 ± 2	0.56 ± 0.01	58 ± 8
45 : 45 : 10 (%w/w)	40	1054 ± 2	0.64 ± 0.01	45 ± 7
45 : 45 : 10 (%w/w)	40	2148 ± 2	0.71 ± 0.02	40 ± 8
45 : 45 : 10 (%w/w)	40	3578 ± 2	0.76 ± 0.02	37 ± 11
45 : 45 : 10 (%w/w)	40	5240 ± 2	0.82 ± 0.02	34 ± 14
72 : 18 : 10 (%w/w)	40	72 ± 2		
72 : 18 : 10 (%w/w)	40	72 ± 2	0.09 ± 0.02	94 ± 13
72 : 18 : 10 (%w/w)	40	72 ± 2	0.19 ± 0.02	93 ± 13
72 : 18 : 10 (%w/w)	40	73 ± 2	0.29 ± 0.02	89 ± 12
72 : 18 : 10 (%w/w)	40	77 ± 2	0.38 ± 0.02	91 ± 12
72 : 18 : 10 (%w/w)	40	109 ± 2	0.47 ± 0.02	81 ± 11
72 : 18 : 10 (%w/w)	40	353 ± 2	0.55 ± 0.01	58 ± 9
72 : 18 : 10 (%w/w)	40	1039 ± 2	0.62 ± 0.01	38 ± 7
72 : 18 : 10 (%w/w)	40	2132 ± 2	0.68 ± 0.02	32 ± 8
72 : 18 : 10 (%w/w)	40	3563 ± 2	0.74 ± 0.02	29 ± 10
72 : 18 : 10 (%w/w)	40	5224 ± 2	0.79 ± 0.02	27 ± 12
16 : 64 : 20 (%w/w)	40	83 ± 2		
16 : 64 : 20 (%w/w)	40	83 ± 2	0.056 ± 0.007	100 ± 12
16 : 64 : 20 (%w/w)	40	83 ± 2	0.111 ± 0.007	99 ± 11
16 : 64 : 20 (%w/w)	40	83 ± 2	0.167 ± 0.007	101 ± 11

(*continued on next page*)

Table A3 (*continued*)

THFA : H2O : MEA	T (°C)	p (mbar)	α (mol CO_2/mol MEA)	ΔH (kJ/mol CO_2)
16 : 64 : 20 (%w/w)	40	83 ± 2	0.223 ± 0.007	101 ± 11
16 : 64 : 20 (%w/w)	40	84 ± 2	0.279 ± 0.007	99 ± 11
16 : 64 : 20 (%w/w)	40	84 ± 2	0.335 ± 0.007	98 ± 11
16 : 64 : 20 (%w/w)	40	86 ± 2	0.390 ± 0.007	97 ± 11
16 : 64 : 20 (%w/w)	40	92 ± 2	0.446 ± 0.006	90 ± 10
16 : 64 : 20 (%w/w)	40	124 ± 2	0.501 ± 0.006	77 ± 8
16 : 64 : 20 (%w/w)	40	283 ± 2	0.554 ± 0.006	56 ± 6
16 : 64 : 20 (%w/w)	40	687 ± 2	0.606 ± 0.006	48 ± 5
16 : 64 : 20 (%w/w)	40	1386 ± 2	0.653 ± 0.007	44 ± 6
16 : 64 : 20 (%w/w)	40	2391 ± 2	0.697 ± 0.007	42 ± 7
16 : 64 : 20 (%w/w)	40	3704 ± 2	0.736 ± 0.009	41 ± 9
16 : 64 : 20 (%w/w)	40	5317 ± 2	0.77 ± 0.01	42 ± 13
40 : 40 : 20 (%w/w)	40	76 ± 2		
40 : 40 : 20 (%w/w)	40	76 ± 2	0.056 ± 0.007	97 ± 11
40 : 40 : 20 (%w/w)	40	77 ± 2	0.112 ± 0.007	92 ± 11
40 : 40 : 20 (%w/w)	40	76 ± 2	0.167 ± 0.007	90 ± 10
40 : 40 : 20 (%w/w)	40	77 ± 2	0.224 ± 0.007	87 ± 10
40 : 40 : 20 (%w/w)	40	77 ± 2	0.280 ± 0.007	89 ± 10
40 : 40 : 20 (%w/w)	40	78 ± 2	0.336 ± 0.007	88 ± 10
40 : 40 : 20 (%w/w)	40	81 ± 2	0.392 ± 0.007	88 ± 10
40 : 40 : 20 (%w/w)	40	93 ± 2	0.449 ± 0.007	83 ± 9
40 : 40 : 20 (%w/w)	40	168 ± 2	0.504 ± 0.006	72 ± 8
40 : 40 : 20 (%w/w)	40	510 ± 2	0.556 ± 0.006	55 ± 6
40 : 40 : 20 (%w/w)	40	1241 ± 2	0.603 ± 0.007	45 ± 6
40 : 40 : 20 (%w/w)	40	2340 ± 2	0.645 ± 0.007	42 ± 7
40 : 40 : 20 (%w/w)	40	3732 ± 2	0.683 ± 0.009	38 ± 8
40 : 40 : 20 (%w/w)	40	5386 ± 2	0.72 ± 0.01	39 ± 12
64 : 16 : 20 (%w/w)	40	65 ± 2		
64 : 16 : 20 (%w/w)	40	64 ± 2	0.056 ± 0.007	92 ± 11
64 : 16 : 20 (%w/w)	40	63 ± 2	0.112 ± 0.007	90 ± 10
64 : 16 : 20 (%w/w)	40	63 ± 2	0.167 ± 0.007	91 ± 10
64 : 16 : 20 (%w/w)	40	64 ± 2	0.223 ± 0.007	91 ± 10
64 : 16 : 20 (%w/w)	40	64 ± 2	0.279 ± 0.007	91 ± 10
64 : 16 : 20 (%w/w)	40	66 ± 2	0.336 ± 0.007	90 ± 10
64 : 16 : 20 (%w/w)	40	71 ± 2	0.391 ± 0.007	91 ± 10
64 : 16 : 20 (%w/w)	40	90 ± 2	0.447 ± 0.007	86 ± 9
64 : 16 : 20 (%w/w)	40	227 ± 2	0.500 ± 0.006	76 ± 9
64 : 16 : 20 (%w/w)	40	814 ± 2	0.549 ± 0.006	54 ± 7
64 : 16 : 20 (%w/w)	40	1902 ± 2	0.590 ± 0.007	42 ± 7
64 : 16 : 20 (%w/w)	40	3317 ± 2	0.629 ± 0.008	36 ± 7
64 : 16 : 20 (%w/w)	40	4915 ± 2	0.66 ± 0.01	32 ± 9
14 : 56 : 30 (%w/w)	40	79 ± 2		
14 : 56 : 30 (%w/w)	40	79 ± 2	0.043 ± 0.004	91 ± 9
14 : 56 : 30 (%w/w)	40	79 ± 2	0.085 ± 0.004	87 ± 9
14 : 56 : 30 (%w/w)	40	79 ± 2	0.127 ± 0.004	86 ± 9
14 : 56 : 30 (%w/w)	40	79 ± 2	0.170 ± 0.004	87 ± 9
14 : 56 : 30 (%w/w)	40	79 ± 2	0.212 ± 0.004	88 ± 9
14 : 56 : 30 (%w/w)	40	80 ± 2	0.255 ± 0.004	88 ± 8
14 : 56 : 30 (%w/w)	40	80 ± 2	0.298 ± 0.004	88 ± 8
14 : 56 : 30 (%w/w)	40	81 ± 2	0.341 ± 0.004	88 ± 8
14 : 56 : 30 (%w/w)	40	82 ± 2	0.383 ± 0.004	89 ± 8
14 : 56 : 30 (%w/w)	40	85 ± 2	0.426 ± 0.004	85 ± 8
14 : 56 : 30 (%w/w)	40	96 ± 2	0.469 ± 0.004	82 ± 7
14 : 56 : 30 (%w/w)	40	160 ± 2	0.512 ± 0.004	69 ± 6
14 : 56 : 30 (%w/w)	40	400 ± 2	0.553 ± 0.004	52 ± 5
14 : 56 : 30 (%w/w)	40	913 ± 2	0.592 ± 0.004	46 ± 5
14 : 56 : 30 (%w/w)	40	1733 ± 2	0.628 ± 0.004	44 ± 5
14 : 56 : 30 (%w/w)	40	2876 ± 2	0.662 ± 0.005	43 ± 6
14 : 56 : 30 (%w/w)	40	4326 ± 2	0.693 ± 0.006	42 ± 8
35 : 35 : 30 (%w/w)	40	70 ± 2		
35 : 35 : 30 (%w/w)	40	70 ± 2	0.042 ± 0.004	96 ± 10
35 : 35 : 30 (%w/w)	40	71 ± 2	0.085 ± 0.004	94 ± 9
35 : 35 : 30 (%w/w)	40	70 ± 2	0.128 ± 0.004	95 ± 9
35 : 35 : 30 (%w/w)	40	71 ± 2	0.170 ± 0.004	96 ± 9
35 : 35 : 30 (%w/w)	40	71 ± 2	0.213 ± 0.004	95 ± 9
35 : 35 : 30 (%w/w)	40	71 ± 2	0.256 ± 0.004	96 ± 9
35 : 35 : 30 (%w/w)	40	72 ± 2	0.299 ± 0.004	96 ± 9
35 : 35 : 30 (%w/w)	40	72 ± 2	0.342 ± 0.004	94 ± 9
35 : 35 : 30 (%w/w)	40	74 ± 2	0.385 ± 0.004	93 ± 9
35 : 35 : 30 (%w/w)	40	78 ± 2	0.427 ± 0.004	89 ± 8
35 : 35 : 30 (%w/w)	40	97 ± 2	0.470 ± 0.004	84 ± 8
35 : 35 : 30 (%w/w)	40	212 ± 2	0.512 ± 0.004	70 ± 6
35 : 35 : 30 (%w/w)	40	636 ± 2	0.552 ± 0.004	53 ± 5
35 : 35 : 30 (%w/w)	40	1478 ± 2	0.587 ± 0.004	46 ± 5
35 : 35 : 30 (%w/w)	40	2688 ± 2	0.620 ± 0.005	42 ± 6

(*continued on next page*)

Table A3 (*continued*)

THFA : H2O : MEA	T (°C)	p (mbar)	α (mol CO_2/mol MEA)	ΔH (kJ/mol CO_2)
35 : 35 : 30 (%w/w)	40	4197 ± 2	0.649 ± 0.006	42 ± 8
56 : 14 : 30 (%w/w)	40	62 ± 2		
56 : 14 : 30 (%w/w)	40	62 ± 2	0.042 ± 0.004	95 ± 10
56 : 14 : 30 (%w/w)	40	61 ± 2	0.085 ± 0.004	93 ± 9
56 : 14 : 30 (%w/w)	40	61 ± 2	0.128 ± 0.004	92 ± 9
56 : 14 : 30 (%w/w)	40	61 ± 2	0.171 ± 0.004	93 ± 9
56 : 14 : 30 (%w/w)	40	62 ± 2	0.213 ± 0.004	93 ± 9
56 : 14 : 30 (%w/w)	40	62 ± 2	0.255 ± 0.004	95 ± 9
56 : 14 : 30 (%w/w)	40	62 ± 2	0.299 ± 0.004	93 ± 9
56 : 14 : 30 (%w/w)	40	63 ± 2	0.342 ± 0.004	93 ± 9
56 : 14 : 30 (%w/w)	40	66 ± 2	0.384 ± 0.004	94 ± 9
56 : 14 : 30 (%w/w)	40	73 ± 2	0.427 ± 0.004	90 ± 8
56 : 14 : 30 (%w/w)	40	105 ± 2	0.470 ± 0.004	85 ± 8
56 : 14 : 30 (%w/w)	40	317 ± 2	0.511 ± 0.004	72 ± 7
56 : 14 : 30 (%w/w)	40	1035 ± 2	0.549 ± 0.004	51 ± 5
56 : 14 : 30 (%w/w)	40	2244 ± 2	0.581 ± 0.005	42 ± 6
56 : 14 : 30 (%w/w)	40	3809 ± 2	0.610 ± 0.006	38 ± 7

Appendix B. Calculating inherent uncertainties

This Appendix B shall outline a methodology to calculate the confidence intervals for the data obtained in this work. The uncertainties shown here come from the inherent inaccuracies of the apparatus used to carry the measurements, and not from any external disturbances nor human mistakes. They are, therefore, the minimum value that these uncertainties could assume given a flawless experimental routine. The inherent inaccuracies of each measurement device used in this study can be seen on Table B1. A list of symbols is shown on Table B2.

Table B1
Uncertainties of measurements.

Parameter		Symbol	Value
Mass		σ(m)	± 0.001 g
Pressure		σ(p)	± 2 mbar
Temperature		σ(T)	± 0.1 K
Power		σ(W)	± 0.1 W
Volume	CO_2 cylinder	V_c	2300 ± 3 mL
	Dry reactor	V_r	270 ± 16 mL

Each solvent is prepared by adding first the diluent(s) and then the amine to a glass bottle. There are at least two mass measurements associated with the calculation of the amine mass fraction, one of the pure amine (m_1) and the other of the whole amount of solvent prepared (m_2). Therefore, the uncertainty of the amine mass fraction can be given by:

$$(m\%) = \frac{m_1}{m_2}$$

$$\sigma^2(m\%) = \left(\frac{1}{m_2}\right)^2 \cdot \sigma^2(m_1) + \left(\frac{m_1}{m_2{}^2}\right)^2 \cdot \sigma^2(m_2) = \left(\frac{m\%}{m_1}\right)^2 \cdot \sigma^2(m_1) + \left(\frac{m\%}{m_2}\right)^2 \cdot \sigma^2(m_2)$$

This solvent is partially fed to the glass reactor and a third measurement is taken (m_3). The mass of amine in the reactor, m_{MEA}, is finally the product of the mass fraction of amine in the original solution and the mass measured inside the reactor:

$$m_{MEA} = m_3 \cdot (m\%)$$

$$\sigma^2(m_{MEA}) = (m\%)^2 \cdot \sigma^2(m_3) + m_3{}^2 \cdot \sigma^2(m\%) = \left(\frac{m_{MEA}}{m_3}\right)^2 \cdot \sigma^2(m_3) + \left(\frac{m_{MEA}}{m\%}\right)^2 \cdot \sigma^2(m\%)$$

$$= \left(\frac{m_{MEA}}{m_3}\right)^2 \cdot \sigma^2(m_3) + \left(\frac{m_{MEA}}{m\%}\right)^2 \cdot \left(\frac{m\%}{m_1}\right)^2 \cdot \sigma^2(m_1) + \left(\frac{m_{MEA}}{m\%}\right)^2 \cdot \left(\frac{m\%}{m_2}\right)^2 \cdot \sigma^2(m_2) = (m_{MEA})^2 \cdot \left[\frac{\sigma^2(m_1)}{m_1{}^2} + \frac{\sigma^2(m_2)}{m_2{}^2} + \frac{\sigma^2(m_3)}{m_3{}^2}\right]$$

Therefore, the relative uncertainty of the amount of amine in the reactor is as big as the sum of the relative uncertainties of each one of the three mass measurements taken.

$$\frac{\sigma^2(m_{MEA})}{m_{MEA}{}^2} = \frac{\sigma^2(m_1)}{m_1{}^2} + \frac{\sigma^2(m_2)}{m_2{}^2} + \frac{\sigma^2(m_3)}{m_3{}^2}$$

Since the scale used in all three measurements has the same accuracy σ(m), this reduces to:

$$\frac{\sigma^2(m_{MEA})}{m_{MEA}{}^2} = \left(\frac{1}{m_1{}^2} + \frac{1}{m_2{}^2} + \frac{1}{m_3{}^2}\right) \cdot \sigma^2(m)$$

The number of mols of amine in the reactor is merely:

Table B2
Symbols used for Appendix B calculations.

Symbol	Meaning
Latin	
$C_{p,CO2}$	Average heat capacity of gaseous CO_2
E_k	Energy exchanged by the calorimeter after injection k
m	Mass
$m\%$	Mass fraction
MM_{MEA}	Molar mass of MEA
n	Number of mols
NI	Number of CO_2 injections
NM	Number of mass measurements
NP	Number of power measurements for numerical integration
p	pressure
R	Ideal gas constant
T	Temperature
t_{NP}	Time between each two measurements for numerical integration
V	Volume
W	Power
Greek	
ρ	Density
$\Delta\alpha_k$	Loading increase in one injection k
ΔH_k	Heat of absorption calculated in one injection k
$\Delta\bar{H}_k$	Heat of absorption per mol of CO_2 absorbed in one injection k
$\Delta n_{CO2,k}$	Mols of CO_2 absorbed in one injection k
Δt_k	Total time over which numerical integration is performed in one injection k
Subscripts	
c	Cylinder
ik	Initial, before injection k
fk	Final, after injection k
r	Reactor
rl	Reactor – liquid phase
rv	Reactor – vapor phase

$$n_{MEA} = \frac{m_{MEA}}{MM_{MEA}}$$

Consequently, the relative uncertainty of the number of mols of amine in the reactor is:

$$\sigma^2(n_{MEA}) = \left(\frac{1}{MM_{MEA}}\right)^2 \cdot \sigma^2(m_{MEA}) = \left(\frac{n_{MEA}}{m_{MEA}}\right)^2 \cdot \sigma^2(m_{MEA})$$

$$\frac{\sigma^2(n_{MEA})}{(n_{MEA})^2} = \sum_{i=1}^{NM} \frac{\sigma^2(m)}{(m_i)^2}$$

where NM is a generalization for the number of mass measurements employed in the experiment. This simple procedure illustrates how error propagation can lead to the uncertainty of an important parameter, the number of mols of amine in the reactor, being dependent of at least three distinct evaluations with the scale. A similar, albeit more complex, result is observed when calculating the number of mols of CO_2 captured by the solvent at any given moment. As mentioned in Section 2, the number of mols of CO_2 absorbed is given by a balance between what leaves the CO_2 cylinders and what remains in the vapor phase of the reactor. That is to say:

$$\Delta n_{CO2,k} = (n_{c,ik} - n_{c,fk}) - (n_{rv,fk} - n_{rv,ik})$$

One needs to calculate the number of mols of CO_2 in both the cylinder and in the vapor phase of the reactor at any given time. It is true that, for the calculations shown in this work, the Peng-Robinson Equation of State is used. However, for simplicity, ideal gas law can be employed for the uncertainty calculations. If ideal gas law applies:

$$\Delta n_{CO2,k} = \left(\frac{p_{c,ik} \cdot V_c}{R \cdot T_{c,ik}} - \frac{p_{c,fk} \cdot V_c}{R \cdot T_{c,fk}}\right) - \left(\frac{p_{r,fk} \cdot V_{rv}}{R \cdot T_{r,fk}} - \frac{p_{r,ik} \cdot V_{rv}}{R \cdot T_{r,ik}}\right)$$

$$\begin{aligned}\frac{\sigma^2(\Delta n_{CO2,k})}{(\Delta n_{CO2,k})^2} &= \left(\frac{n_{c,ik}}{\Delta n_{CO2,k}}\right)^2 \cdot \left[\frac{\sigma^2(p)}{(p_{c,ik})^2} + \frac{\sigma^2(T)}{(T_{c,ik})^2} + \frac{\sigma^2(V_c)}{(V_c)^2}\right] + \left(\frac{n_{c,fk}}{\Delta n_{CO2,k}}\right)^2 \cdot \left[\frac{\sigma^2(p)}{(p_{c,fk})^2} + \frac{\sigma^2(T)}{(T_{c,fk})^2} + \frac{\sigma^2(V_c)}{(V_c)^2}\right] + \left(\frac{n_{rv,ik}}{\Delta n_{CO2,k}}\right)^2 \\ &\cdot \left[\frac{\sigma^2(p)}{(p_{r,ik})^2} + \frac{\sigma^2(T)}{(T_{r,ik})^2} + \frac{\sigma^2(V_{rv})}{(V_{rv})^2}\right] + \left(\frac{n_{rv,fk}}{\Delta n_{CO2,k}}\right)^2 \cdot \left[\frac{\sigma^2(p)}{(p_{r,fk})^2} + \frac{\sigma^2(T)}{(T_{r,fk})^2} + \frac{\sigma^2(V_{rv})}{(V_{rv})^2}\right]\end{aligned}$$

The uncertainty of the number of mols of CO_2 absorbed depends on four pressure measurements and four temperature measurements, all with the same accuracy σ(p) and σ(T) respectively. It also depends on the uncertainty of the volume of the CO_2 cylinder, which is naturally constant and given by the calibration of the apparatus. Finally, it depends on the uncertainty of the volume of vapor in the reactor. This is the volume of the dry reactor

minus the volume occupied by liquid. Assuming that the density of the liquid is given with great precision and changes little upon CO_2 absorption, this means that:

$$\sigma^2(V_{rv}) = \sigma^2(V_r) + \frac{\sigma^2(m)}{(\rho_{rl})^2}$$

With these results, the amount of CO_2 loaded at each injection k is merely:

$$\Delta\alpha_k = \frac{\Delta n_{CO2,k}}{n_{MEA}}$$

So that the uncertainty of this extra loading is given by:

$$\sigma^2(\Delta\alpha_k) = \left(\frac{1}{n_{MEA}}\right)^2 \cdot \sigma^2(\Delta n_{CO2,k}) + \left(\frac{\Delta n_{CO2,k}}{{n_{MEA}}^2}\right)^2 \cdot \sigma^2(n_{MEA}) = (\Delta\alpha_k)^2 \cdot \frac{\sigma^2(\Delta n_{CO2,k})}{(\Delta n_{CO2,k})^2} + (\Delta\alpha_k)^2 \cdot \frac{\sigma^2(n_{MEA})}{(n_{MEA})^2}$$

$$\frac{\sigma^2(\Delta\alpha_k)}{(\Delta\alpha_k)^2} = \frac{\sigma^2(\Delta n_{CO2,k})}{(\Delta n_{CO2,k})^2} + \frac{\sigma^2(n_{MEA})}{(n_{MEA})^2}$$

Naturally, the uncertainty of the overall loading propagates from injection to injection:

$$\sigma^2(\alpha) = \sum_{i=1}^{NI} \sigma^2(\Delta\alpha_i)$$

Despite all the aforementioned error propagation, the confidence intervals for the loadings obtained in the course of the experiments carried in this work are quite good (see Tables A1, A2 and A3). That happens because the accuracies of every mass, pressure and temperature measurements are reasonably high.

The heat exchanged by the calorimeter after CO_2 injection is calculated by numerical integration of the power measured in the apparatus over time, for as long as it takes the reactor to return to its set point temperature. This integration is performed by the ChemiCall software. In other words:

$$E_k = \int W(t) \cdot dt$$

Assuming that a composite Simpson rule is employed for the numerical integration and that the total time Δt is divided in NP-1 identical time intervals of span t_{NP}:

$$\int W(t) \cdot dt \frac{\Delta t_k}{3 \cdot NP} \cdot \sum_{i=1}^{NP/2} W_{2 \cdot i-2} + 4 \cdot W_{2 \cdot i-1} + W_{2 \cdot i}$$

Since each power measurement has the same uncertainty σ(W):

$$\sigma^2(E_k) = \left(\frac{\Delta t_k}{3 \cdot NP}\right)^2 \cdot \sum_{i=1}^{NP/2} \sigma^2(W) + 16 \cdot \sigma^2(W) + \sigma^2(W) = \left(\frac{\Delta t_k}{3 \cdot NP}\right)^2 \cdot \sum_{i=1}^{NP/2} 18 \cdot \sigma^2(W) = \frac{NP}{2} \cdot \left(\frac{\Delta t_k}{3 \cdot NP}\right)^2 \cdot 18 \cdot \sigma^2(W) = \frac{{\Delta t_k}^2}{NP} \cdot \sigma^2(W)$$

The quotient of Δt by NP is merely the time interval between each measurement used by the numerical integration. This is standard for all experiments and equals $t_{NP} = 10$ s. The total time spent for the system to return to its set point, Δt, varies from experiment to experiment. In average, it has been observed that $\Delta t = 2100$ s (35 min) are necessary for most solvents employed in this particular study. This returns $\sigma(E_k) \approx 210$ J.

$$\sigma^2(E_k) = \Delta t_k \cdot t_{NP} \cdot \sigma^2(W)$$

Not all power measured by the calorimeter concerns the heat of absorption of CO_2. A parcel of the heat is removed by the warming up of CO_2 from its cylinder temperature (typically around 20 °C) to the reactor temperature, whereas some heat is generated by the compression of the vapour phase of the reactor upon addition of CO_2. Therefore:

$$E_k = \Delta H_k - C_{p,CO2} \cdot (T_{r,fk} - T_{c,ik}) + V_{rv} \cdot (p_{r,fk} - p_{r,ik})$$

$$\sigma^2(\Delta H_k) = \sigma^2(E_k) + 2 \cdot {C_{p,CO2}}^2 \cdot \sigma^2(T) + 2 \cdot {V_{rv}}^2 \cdot \sigma^2(p) + (p_{r,fk} - p_{r,ik})^2 \cdot \sigma^2(V_{rv})$$

In the previous equations, an average heat capacity for gaseous CO_2 was employed. This is for illustration purposes only, as in reality a polynomial expression for $C_{P,CO2}$ was obtained in [46] and used for all relevant calculations. Finally, the uncertainty of the differential heat of absorption is obtained by:

$$\Delta\bar{H}_k = \frac{\Delta H_k}{\Delta\alpha_k}$$

$$\sigma^2(\Delta\bar{H}_k) = \left(\frac{\Delta\bar{H}_k}{\Delta\alpha_k}\right)^2 \cdot \sigma^2(\Delta\alpha_k) + \left(\frac{\Delta\bar{H}_k}{\Delta H_k}\right)^2 \cdot \sigma^2(\Delta H_k) = \Delta\bar{H}_k^2 \cdot \left[\frac{\sigma^2(\Delta n_{CO2,k})}{(\Delta n_{CO2,k})^2} + \frac{\sigma^2(n_{MEA})}{(n_{MEA})^2} + \frac{\sigma^2(\Delta H_k)}{(\Delta H_k)^2}\right]$$

$$\frac{\sigma^2(\Delta\bar{H}_k)}{(\Delta\bar{H}_k)^2} = \frac{\sigma^2(\Delta n_{CO2,k})}{(\Delta n_{CO2,k})^2} + \frac{\sigma^2(n_{MEA})}{(n_{MEA})^2} + \frac{\sigma^2(\Delta H_k)}{(\Delta H_k)^2}$$

One might now discuss the way that these calorimetry experiments are carried. Typically, one is interested in obtaining a curve for the differential heat of absorption of the solvent. This is done by effecting very small injections of CO_2 and evaluating the power required to return the instrument back to its set point. Nevertheless, the time it takes to happen is not uniquely a function of how much CO_2 was introduced. It depends also on the transport properties of the solvent, the robustness of the temperature controller and the dimensions of the apparatus itself. A consequence of

this is that bigger CO_2 injections reveal the heat of absorption with relatively more accuracy. Considering Fig. 4 for example, the confidence intervals for aqueous MEA 30 %w/w are tighter than those of methanol + MEA 30 %w/w simply because the former experiment was carried with fewer injections (8) than the latter (19). This has been a lesson learned on the operation of calorimetry measurements. Similarly, an apparatus such as the calorimeter employed by Kim and Svendsen [10] is able to produce data with more accuracy precisely because of its size. In spite of the time required for reaching the set point being similar in both instruments, their equipment requires about 10 times more solvent than the small calorimeter used in this study, meaning its measured uncertainties could be even 10 times smaller than the ones shown here.

Some final words should be said about two of the most objectionable assumptions made while treating the data. The first one is that the density of the solvent does not change perceptively upon CO_2 absorption. Without this assumption, the vapor volume in the reactor during the course of the experiments is unknown and no loadings can be calculated. The second one is that the vapor pressure of the solvent is independent of loading, i.e. that addition of CO_2 to the medium does not promote the volatilization of the solvent. This can be somewhat dismissed for non-volatile solvents, but the situation is problematic when dealing with methanolic solutions for example. Furthermore, since this work particularly deals with mixtures between organic diluents and amines, it is imaginable that the activities of all solvent molecules increase more upon electrolyte formation than those of ordinary aqueous solutions [27]. To address both these issues, the solution remaining in the reactor after final injection is sampled and titrated. If the loading obtained through titration is within ± 3% of that calculated by molar balance, all points are validated and the results are the ones shown in Tables A1, A2 and A3. Otherwise, the experiment is repeated. The agreement between titration and molar balance results was overall good in these experiments, and this methodology has been proved valid for water-lean solvents.

Appendix C. Reproducibility and validation

The discussion that follows in Appendix C will rely on the methodology described in this paragraph. Experiments with aqueous MEA 30 %w/w were carried at 40 °C several times in a row, forming datasets #1–#6. Using datasets #1–#6, equations were fitted to reflect the variation of total pressure and differential heat of absorption with loading employing, respectively, a 5th order polynomial and a generalized logistic function. This fitting is performed in a way that the average absolute relative deviation (AARD) between the experimental dataset **x** containing NE points and the model **x*** is minimized, as the equation below shows.

$$AARD(\%) = \frac{100\%}{NE} \cdot \sum_{i=1}^{NE} \left| \frac{x_i - x_i^*}{x_i} \right|$$

The quality of the reproducibility of an experiment is then represented by this AARD. If its value is too high, that means the reproducibility is weak. If it is close to null, that means all datasets can be laid on the same curve. The value of p_{CO2} of aqueous MEA is checked against literature data of Jou et al. [14] and Aronu et al. [15] for evaluation of the repeatability of the measurements. Additionally, three experiments with NMP + MEA 30 %w/w and three experiments with THFA + MEA 30 %w/w at 40 °C were performed to evaluate the reproducibility of the calorimetric procedure with regards to water-lean solvents.

Fig. C1 shows the reproducibility plot for total pressure versus loading for aqueous MEA 30 %w/w at 313 K. The AARD obtained with the 5th order polynomial is of 8.4% for the six distinct datasets. As it can be seen in Fig. C1, the reproducibility of the VLE curves is overall quite good, and the somewhat high value of AARD = 8.4% comes about only because, at very small pressures, small fluctuations generate high relative deviations. If only data gathered below 10 kPa is considered, the AARD would be of 11.9%, while that above 10 kPa would have an AARD of merely 2.8%.

Fig. C2 shows the validation for p_{CO2} obtained in the calorimeter against literature data [14,15]. It must be noticed that the procedure with the calorimeter does not measure p_{CO2} directly, but only the total pressure in the reactor, meaning that p_{CO2} must be recovered by subtraction of the partial pressure of the solvent. Because of error propagation, this means that p_{CO2} is more accurate the higher the pressure measured. Therefore, in Fig. C2, a good agreement is seen between the p_{CO2} obtained in the calorimeter and that measured by Aronu et al. [15] at loadings above $\alpha \approx 0.50$. The deviations between datasets #1–#6 and literature data are not bigger than the deviations between the two sources themselves.

The procedure of measuring total pressure instead of CO_2 partial pressure could be particularly problematic with increasing temperatures, where volatilization of both amine and diluent can interfere in the calculation of vapor-liquid equilibrium curves, particularly at higher loadings. However, as it can be seen on Fig. C3, the values obtained in the calorimeter seems to fit literature data from Aronu et al. [15] as adequately at 313 K as at 353 K and 393 K. Therefore, one could conclude that the effects of volatilization are negligible in the span of temperatures and compositions analyzed in this work.

Regarding ΔH, datasets #2 and #5 had to be excluded due to showing an odd behavior. In the remaining datasets, the overall heat of absorption

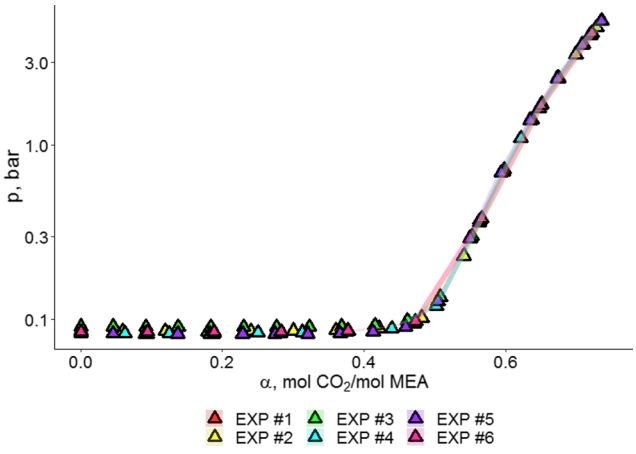

Fig. C1. Reproducibility of total pressure of aqueous MEA 30 %w/w at 313 K.

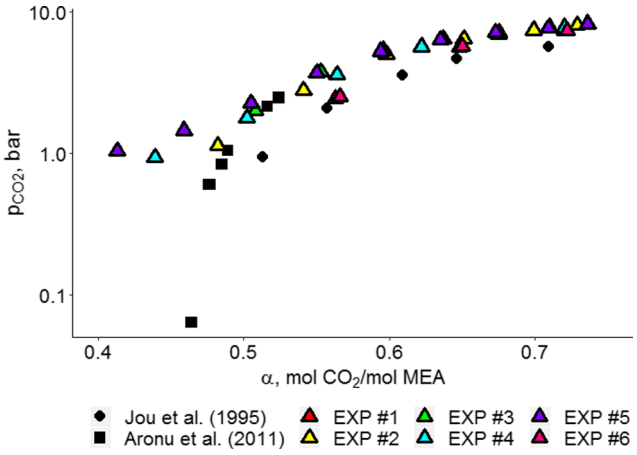

Fig. C2. Validation of p_{CO2} of aqueous MEA 30 %w/w at 313 K with literature data.

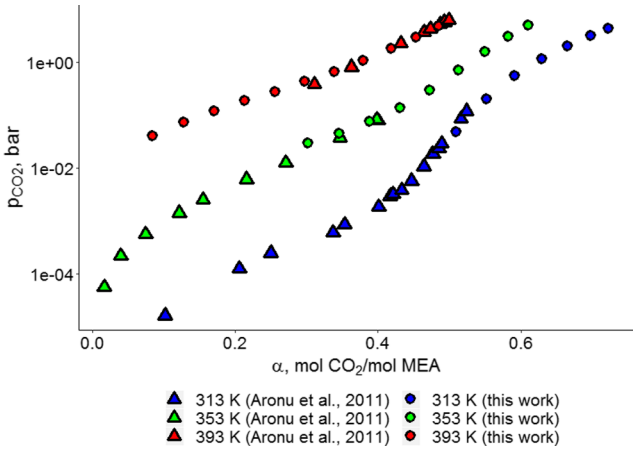

Fig. C3. Validation of p_{CO2} of aqueous MEA 30 %w/w at different temperatures against data from [15].

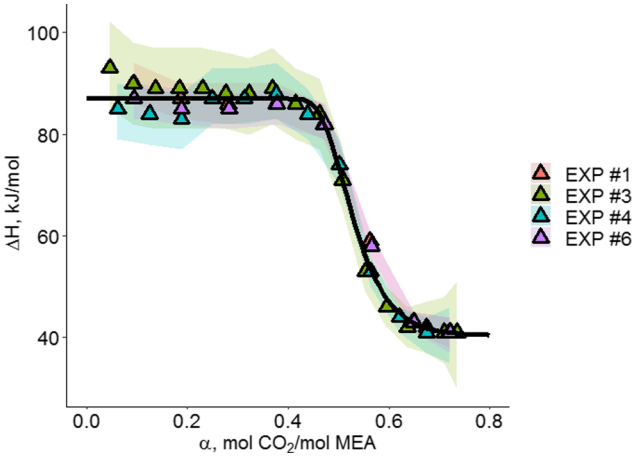

Fig. C4. Reproducibility for ΔH of aqueous MEA 30 %w/w at 313 K.

conforms to a value very similar to that reported by other authors [10,47] during the chemical reaction interval ($\alpha < 0.50$). While Kim et al. [47] report a mean heat of absorption of around 84.3 kJ/mol CO_2, experiments #1, #3, #4 and #6 have produced an average of 87 kJ/mol CO_2. With this, one could say that the heat of absorption measured in the small calorimeter can be validated against literature data. Moreover, excluding datasets #2 and #5, the calculated AARD is of 2.0%. This can be seen in Fig. C4.

Results for the three experiments with the solvents NMP + MEA and THFA + MEA 30 %w/w are shown in Fig. C5. Their AARD are respectively 2.8 and 3.8%. Though these values are higher than those of aqueous MEA 30 %w/w, it is important to notice that the reproducibility found for all solvents is similar to the accuracy of the experiment itself. Therefore, the confidence intervals given in Tables A1, A2 and A3 are deemed proper for the representation of the data obtained in this work.

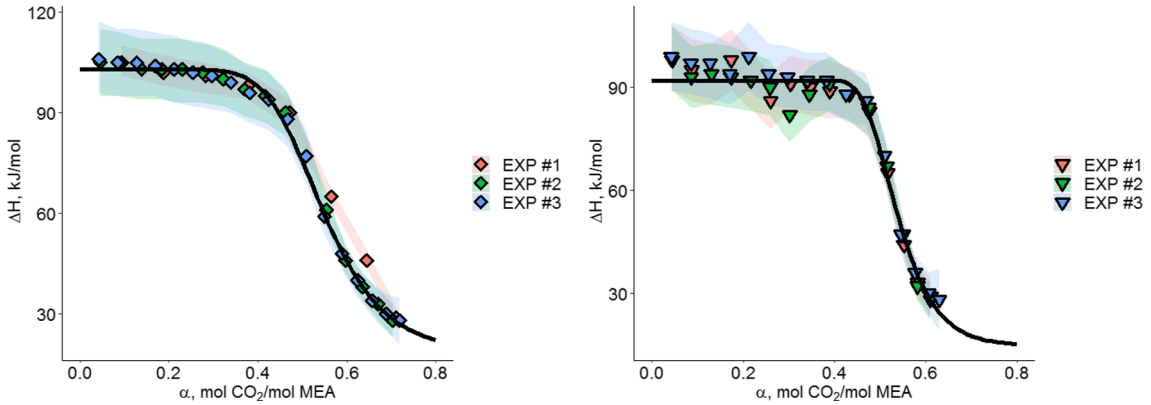

Fig. C5. Reproducibility for ΔH of NMP (left) and THFA (right) + MEA 30 %w/w at 313 K.

Appendix D. Supplementary material

Supplementary data to this article can be found online at https://doi.org/10.1016/j.seppur.2019.115883.

References

[1] G.T. Rochelle, Amine scrubbing for CO2 capture, Science 325 (2009) 1652–1654, https://doi.org/10.1126/science.1176731.

[2] A.L. Kohl, R.B. Nielsen, A.L. Kohl, R.B. Nielsen, Alkanolamines for hydrogen sulfide and carbon dioxide removal, Gas Purif. (1997) 40–186, https://doi.org/10.1016/B978-088415220-0/50002-1.

[3] I.M. Bernhardsen, H.K. Knuutila, A review of potential amine solvents for CO2 absorption process: Absorption capacity, cyclic capacity and pKa, Int. J. Greenh. Gas Control. 61 (2017) 27–48, https://doi.org/10.1016/J.IJGGC.2017.03.021.

[4] S. Singto, T. Supap, R. Idem, P. Tontiwachwuthikul, S. Tantayanon, The effect of chemical structure of newly synthesized tertiary amines used for the post combustion capture process on carbon dioxide (CO2): Kinetics of CO2 absorption using the stopped-flow apparatus and regeneration, and heat input of CO2 regeneration, Energy Procedia 114 (2017) 852–859, https://doi.org/10.1016/J.EGYPRO.2017.03.1227.

[5] R.J. Macgregor, A.E. Mather, Equilibrium solubility of H_2S and CO_2 and their mixtures in a mixed solvent, Can. J. Chem. Eng. 69 (1991) 1357–1366, https://doi.org/10.1002/cjce.5450690618.

[6] M. Kriebel, Improved Amisol Process for gas purification, Energy Prog.; (United States) 4 (3) (1984) https://www.osti.gov/biblio/6121828-improved-amisol-process-gas-purification (accessed March 5, 2019).

[7] A.L. Kohl, R.B. Nielsen, A.L. Kohl, R.B. Nielsen, Physical solvents for acid gas removal, Gas Purif. (1997) 1187–1237, https://doi.org/10.1016/B978-088415220-0/50014-8.

[8] T.A. Semenova, I.L. Leites (Eds.), The Purification of Technological Gases, 2nd ed., Chimia, Moscow, 1977.

[9] B. Gwinner, D. Roizard, F. Lapicque, F. Eric, R. Cadours, P. Boucot, C. Pierre-Louis, CO2 capture in flue gas: Semiempirical approach to select a potential physical solvent, 2006. doi:10.1021/IE0580396.

[10] I. Kim, H.F. Svendsen, Heat of absorption of carbon dioxide (CO2) in monoethanolamine (MEA) and 2-(aminoethyl)ethanolamine (AEEA) solutions, 2007, doi:10.1021/IE0616489.

[11] H. Svensson, V. Zejnullahu Velasco, C. Hulteberg, H.T. Karlsson, Heat of absorption of carbon dioxide in mixtures of 2-amino-2-methyl-1-propanol and organic solvents, Int. J. Greenh. Gas Control. 30 (2014) 1–8, https://doi.org/10.1016/J.IJGGC.2014.08.022.

[12] S. Evjen, A. Fiksdahl, D.D.D. Pinto, H.K. Knuutila, New polyalkylated imidazoles tailored for carbon dioxide capture, Int. J. Greenh. Gas Control. 76 (2018) 167–174, https://doi.org/10.1016/j.ijggc.2018.06.017.

[13] S. Evjen, R. Wanderley, A. Fiksdahl, H.K. Knuutila, Viscosity, density, and volatility of binary mixtures of imidazole, 2-methylimidazole, 2,4,5-trimethylimidazole, and 1,2,4,5-tetramethylimidazole with water, J. Chem. Eng. Data. 64 (2019) 507–516, https://doi.org/10.1021/acs.jced.8b00674.

[14] F.-Y. Jou, A.E. Mather, F.D. Otto, The solubility of CO_2 in a 30 mass percent monoethanolamine solution, Can. J. Chem. Eng. 73 (1995) 140–147, https://doi.org/10.1002/cjce.5450730116.

[15] U.E. Aronu, S. Gondal, E.T. Hessen, T. Haug-Warberg, A. Hartono, K.A. Hoff, H.F. Svendsen, Solubility of CO2 in 15, 30, 45 and 60 mass% MEA from 40 to 120 °C and model representation using the extended UNIQUAC framework, Chem. Eng. Sci. 66 (2011) 6393–6406, https://doi.org/10.1016/J.CES.2011.08.042.

[16] H.K. Knuutila, Å. Nannestad, Effect of the concentration of MAPA on the heat of absorption of CO2 and on the cyclic capacity in DEEA-MAPA blends, Int. J. Greenh. Gas Control. 61 (2017) 94–103, https://doi.org/10.1016/J.IJGGC.2017.03.026.

[17] P. Usubharatana, P. Tontiwachwuthikul, Enhancement factor and kinetics of CO2 capture by MEA-methanol hybrid solvents, Energy Procedia 1 (2009) 95–102, https://doi.org/10.1016/J.EGYPRO.2009.01.015.

[18] K. Fu, W. Rongwong, Z. Liang, Y. Na, R. Idem, P. Tontiwachwuthikul, Experimental analyses of mass transfer and heat transfer of post-combustion CO2 absorption using hybrid solvent MEA–MeOH in an absorber, Chem. Eng. J. 260 (2015) 11–19, https://doi.org/10.1016/J.CEJ.2014.08.064.

[19] J. Banasiak, Solubility of carbon dioxide in methanol-monoethanolamine mixtures, gaz, Woda i Tech. Sanit. 55 (1981) 196–199.

[20] P. Usubharatana, A. Veawab, A. Aroonwilas, P. Tontiwachwuthikul, Mass transfer performance of CO2 capture by aqueous hybrid MEA-methanol in packed absorber, in: 2006 IEEE EIC Clim. Chang. Conf., IEEE, 2006, pp. 1–7. doi:10.1109/EICCCC.2006.277215.

[21] F.J. Tamajón, E. Álvarez, F. Cerdeira, D. Gómez-Díaz, CO2 absorption into N-methyldiethanolamine aqueous-organic solvents, Chem. Eng. J. 283 (2016) 1069–1080, https://doi.org/10.1016/J.CEJ.2015.08.065.

[22] B.B. Woertz, Experiments with solvent-amine-water for removing CO2 from gas, Can. J. Chem. Eng. 50 (1972) 425–427, https://doi.org/10.1002/cjce.5450500321.

[23] O.R. Rivas, J.M. Prausnitz, Sweetening of sour natural gases by mixed-solvent absorption: Solubilities of ethane, carbon dioxide, and hydrogen sulfide in mixtures of physical and chemical solvents, AIChE J. 25 (1979) 975–984, https://doi.org/10.1002/aic.690250608.

[24] C. Alvarez-Fuster, N. Midoux, A. Laurent, J.C. Charpentier, Chemical kinetics of the reaction of CO2 with amines in pseudo m–nth order conditions in polar and viscous organic solutions, Chem. Eng. Sci. 36 (1981) 1513–1518, https://doi.org/10.1016/0009-2509(81)85112-3.

[25] F. Murrieta-Guevara, A. Trejo Rodriguez, Solubility of carbon dioxide, hydrogen sulfide, and methane in pure and mixed solvents, J. Chem. Eng. Data. (1984) 456–460, https://doi.org/10.1021/je00038a027 29.

[26] I.L. Leites, Thermodynamics of CO2 solubility in mixtures monoethanolamine with organic solvents and water and commercial experience of energy saving gas purification technology, Energy Convers. Manag. 39 (1998) 1665–1674, https://doi.org/10.1016/S0196-8904(98)00076-4.

[27] R.R. Wanderley, Y. Yuan, G.T. Rochelle, H.K. Knuutila, CO2 solubility and mass transfer in water-lean solvents, Chem. Eng. Sci. 202 (2019) 403–416, https://doi.org/10.1016/J.CES.2019.03.052.

[28] X. Gui, Z. Tang, W. Fei, Solubility of CO_2 in alcohols, glycols, ethers, and ketones at high pressures from (288.15 to 318.15) K, J. Chem. Eng. Data. 56 (2011) 2420–2429, https://doi.org/10.1021/je101344v.

[29] W.G. Gorman, G.D. Hall, Dielectric constant correlations with solubility and solubility parameters, J. Pharm. Sci. 53 (1964) 1017–1020, https://doi.org/10.1002/jps.2600530905.

[30] E. Sada, H. Kumazawa, Z.Q. Han, H. Matsuyama, Chemical kinetics of the reaction of carbon dioxide with ethanolamines in nonaqueous solvents, AIChE J. 31 (1985) 1297–1303, https://doi.org/10.1002/aic.690310808.

[31] E. Sada, H. Kumazawa, Y. Osawa, M. Matsuura, Z.Q. Han, Reaction kinetics of carbon dioxide with amines in non-aqueous solvents, Chem. Eng. J. 33 (1986) 87–95, https://doi.org/10.1016/0300-9467(86)80038-7.

[32] E.S. Hamborg, C. van Aken, G.F. Versteeg, The effect of aqueous organic solvents on the dissociation constants and thermodynamic properties of alkanolamines, Fluid Phase Equilib. 291 (2010) 32–39, https://doi.org/10.1016/J.FLUID.2009.12.007.

[33] X. Li, Y. Jiang, G. Han, D. Deng, Investigation of the solubilities of carbon dioxide in some low volatile solvents and their thermodynamic properties, J. Chem. Eng. Data. 61 (2016) 1254–1261, https://doi.org/10.1021/acs.jced.5b00893.

[34] P. Wothers, N. Greeves, S. Warren, J. Clayden, Org. Chem. (2001).

[35] T.L. Brown, Quantitative correlation of the infrared O-H absorption intensity in aliphatic alcohols with substituent constants, J. Am. Chem. Soc. 80 (1958) 6489–6491 (accessed May 2, 2019), https://pubs.acs.org/doi/pdf/10.1021/ja01557a005.

[36] P.T. Narasimhan, Dipole moments of some heterocyclic compounds, J. Indian Inst. Sci. 37 (1954) 30–34 (accessed May 2, 2019), http://journal.library.iisc.ernet.in/index.php/iisc/article/view/4089/4757.
[37] A.A. Maryott, E.R. Smith, Table of dielectric constants of pure liquids, 1951.
[38] S. Yamamoto, H. Yamada, T. Higashii, Development of chemical CO2 solvent for high pressure CO2 capture (2): Addition effects of non-aqueous media on amine solutions, Energy Procedia 63 (2014) 1963–1971, https://doi.org/10.1016/J.EGYPRO.2014.11.209.
[39] R.R. Wanderley, S. Evjen, D.D.D. Pinto, H.K. Knuutila, The Salting-out effect in some physical absorbents for CO2 capture, in: Chem. Eng. Trans., 2018: pp. 97–102. doi:10.3303/CET1869017.
[40] J. Oexmann, A. Kather, Minimising the regeneration heat duty of post-combustion CO2 capture by wet chemical absorption: The misguided focus on low heat of absorption solvents, Int. J. Greenh. Gas Control. 4 (2010) 36–43, https://doi.org/10.1016/J.IJGGC.2009.09.010.
[41] Dortmund Data Bank, DDBST GmbH, 2019. http://www.ddbst.com/ (accessed June 23, 2019).
[42] J.N. Knudsen, J.N. Jensen, P. Vilhelmsen, First year operation experience with a 1 t / h CO2 absorption pilot plant at Esbjerg coal-fired power plant, 2007. www.co2castor.com (accessed April 26, 2019).
[43] H.M. Kvamsdal, G. Haugen, H.F. Svendsen, A. Tobiesen, H. Mangalapally, A. Hartono, T. Mejdell, Modelling and simulation of the Esbjerg pilot plant using the Cesar 1 solvent, Energy Procedia 4 (2011) 1644–1651, https://doi.org/10.1016/J.EGYPRO.2011.02.036.
[44] L. Raynal, P. Alix, P.-A. Bouillon, A. Gomez, M. le F. de Nailly, M. Jacquin, J. Kittel, A. di Lella, P. Mougin, J. Trapy, The DMX^{TM} process: An original solution for lowering the cost of post-combustion carbon capture, Energy Procedia 4 (2011) 779–786, https://doi.org/10.1016/J.EGYPRO.2011.01.119.
[45] Y. Yuan, G.T. Rochelle, CO2 absorption rate in semi-aqueous monoethanolamine, Chem. Eng. Sci. 182 (2018) 56–66, https://doi.org/10.1016/J.CES.2018.02.026.
[46] Joseph M. Smith, Hendrick C. Van Ness, M.M., Abbott, Introduction to Chemical Engineering Thermodynamics, McGraw-Hill, 2005.
[47] I. Kim, K.A. Hoff, T. Mejdell, Heat of absorption of CO2 with aqueous solutions of MEA: new experimental data, Energy Procedia 63 (2014) 1446–1455, https://doi.org/10.1016/J.EGYPRO.2014.11.154.